Published in final edited form as:
*Anesth Analg*. 2014 March ; 118(3): 525–544. doi:10.1213/ANE.0000000000000088.

# Perioperative Assessment of Myocardial Deformation

**Andra E. Duncan, MD**,
Departments of Cardiothoracic Anesthesia, Outcomes Research, and Cardiovascular Medicine, Cleveland Clinic, Cleveland, Ohio

**Andrej Alfirevic, MD**,
Departments of Cardiothoracic Anesthesia, Outcomes Research, and Cardiovascular Medicine, Cleveland Clinic, Cleveland, Ohio

**Daniel I. Sessler, MD**,
Departments of Cardiothoracic Anesthesia, Outcomes Research, and Cardiovascular Medicine, Cleveland Clinic, Cleveland, Ohio

**Zoran B. Popovic, MD**, and
Departments of Cardiothoracic Anesthesia, Outcomes Research, and Cardiovascular Medicine, Cleveland Clinic, Cleveland, Ohio

**James D. Thomas, MD**
Departments of Cardiothoracic Anesthesia, Outcomes Research, and Cardiovascular Medicine, Cleveland Clinic, Cleveland, Ohio

## Abstract

Evaluation of left ventricular performance improves risk assessment and guides anesthetic decisions. However, the most common echocardiographic measure of myocardial function, the left ventricular ejection fraction (LVEF), has important limitations. LVEF is limited by subjective interpretation which reduces accuracy and reproducibility, and LVEF assesses global function

Corresponding Author: Andra E. Duncan, MD, Department of Cardiothoracic Anesthesia, Cleveland Clinic, 9500 Euclid Avenue/J4, Cleveland, OH 44195, Phone: 216-445-2372, FAX: 216-445-2536, duncana@ccf.org.

The authors declare no conflicts of interest.

Reprints will not be available from the authors.

**DISCLOSURES:**
**Name:** Andra E. Duncan, MD
**Contribution:** This author helped design the study, conduct the study, analyze the data, and write the manuscript
**Attestation:** Andra E. Duncan approved the final manuscript
**Name:** Andrej Alfirevic, MD
**Contribution:** This author helped write the manuscript
**Attestation:** Andrej Alfirevic approved the final manuscript
**Name:** Daniel I. Sessler, MD
**Contribution:** This author helped write the manuscript
**Attestation:** Daniel I. Sessler approved the final manuscript
**Name:** Zoran B. Popovic, MD
**Contribution:** This author helped write the manuscript
**Attestation:** Zoran B. Popovic approved the final manuscript
**Name:** James D. Thomas, MD
**Contribution:** This author helped design the study, conduct the study, analyze the data, and write the manuscript
**Attestation:** James Thomas approved the final manuscript
**This manuscript was handled by:** Martin J. London, MD

without characterizing regional myocardial abnormalities. An alternative objective echocardiographic measure of myocardial function is thus needed. Myocardial deformation analysis, which performs quantitative assessment of global and regional myocardial function, may be useful for perioperative care of surgical patients. Myocardial deformation analysis evaluates left ventricular mechanics by quantifying strain and strain rate. Strain describes percent change in myocardial length in the longitudinal (from base to apex) and circumferential (encircling the short-axis of the ventricle) direction and change in thickness in the radial direction. Segmental strain describes regional myocardial function. Strain is a negative number when the ventricle shortens longitudinally or circumferentially and is positive with radial thickening. Reference values for normal longitudinal strain from a recent meta-analysis using transthoracic echocardiography are (mean ± SD) −19.7 ± 0.4%, while radial and circumferential strain are 47.3 ± 1.9 and −23.3 ± 0.7%, respectively. The speed of myocardial deformation is also important and is characterized by strain rate. Longitudinal systolic strain rate in healthy subjects averages $-1.10 \pm 0.16\ sec^{-1}$. Assessment of myocardial deformation requires consideration of both strain (change in deformation), which correlates with LVEF, and strain rate (speed of deformation), which correlates with rate of rise of left ventricular pressure (dP/dt). Myocardial deformation analysis also evaluates ventricular relaxation, twist, and untwist, providing new and noninvasive methods to assess components of myocardial systolic and diastolic function. Myocardial deformation analysis is based on either Doppler or a non-Doppler technique, called speckle-tracking echocardiography. Myocardial deformation analysis provides quantitative measures of global and regional myocardial function for use in the perioperative care of the surgical patient. For example, coronary graft occlusion after coronary artery bypass grafting is detected by an acute reduction in strain in the affected coronary artery territory. In addition, assessment of left ventricular mechanics detects underlying myocardial pathology before abnormalities become apparent on conventional echocardiography. Certainly, patients with aortic regurgitation demonstrate reduced longitudinal strain before reduction in LVEF occurs, which allows detection of subclinical left ventricular dysfunction and predicts increased risk for heart failure and impaired myocardial function after surgical repair. In this review we describe the principles, techniques, and clinical application of myocardial deformation analysis.

## Introduction

Left ventricular (LV) dysfunction increases risk for cardiovascular complications and death after cardiac[1] and noncardiac surgery.[2–4] Evaluation of LV performance thus impacts risk assessment and guides anesthetic decisions. However, the most common echocardiographic measure of myocardial function, the LV ejection fraction (LVEF), has numerous limitations, including subjective interpretation[5,6] and dependence on ventricular loading conditions and heart rate. Furthermore, considerable operator experience with conventional two-dimensional (2D) echocardiography is required to identify regional myocardial dysfunction.[6] A reliable and reproducible quantitative measure of regional and global myocardial function could improve preoperative risk stratification and guide anesthetic management when acute changes in myocardial function occur.

Myocardial deformation analysis is an echocardiographic approach to quantify global and regional myocardial function, thus allowing assessment of perioperative systolic and

diastolic ventricular function. This technique evaluates myocardial kinesis, based on velocity gradients measured by Doppler or displacement of speckles from 2D images in 3 directions/axes: longitudinal shortening (from base to apex), circumferential shortening (encircling the short-axis of the ventricle), and radial thickening (in the transverse direction from endocardium to epicardium) (Fig. 1). Myocardial deformation analysis quantifies change of regional myocardial segments in these three dimensions using strain (ε) and strain rate (SR) which provide semiobjective, quantitative measures of global and regional myocardial function.[7–9]

Quantitative evaluation of cardiac mechanics, including myocardial velocities[10] and strain,[6,11–14] has been reviewed in the medical literature including a consensus statement on indications and methodology of strain from the American Society of Echocardiography and European Association of Echocardiography.[11,12] Our review will summarize principles and applications of myocardial deformation, with particular reference to intraoperative transesophageal echocardiography (TEE).

## Myocardial strain

Strain is a unitless measure, defined as the proportional change in length between two time points, which is described in unit measurements of percent (%). For a myocardial segment, Lagrangian strain is the fractional change in length of an object compared to its original length. Lagrangian strain is described by the equation:

$$\varepsilon = (L - L_0)/L_0 = \Delta L/L_0,$$

where ε = myocardial strain, L= length at end-systole, $L_0$ = initial length measured at end-diastole (Fig. 2).[6,14] Strain can also be calculated as instantaneous (Eulerian or natural) strain, which describes strain relative to its length at a previous moment in time, rather than relative to its original length. Natural strain is calculated as:

$$\text{natural Strain} = \ln(1 + \text{Lagrangian Strain})$$

where ln is the natural logarithm. This review will refer to Lagrangian strain as “strain” unless otherwise noted.

During systole when the LV shortens in the longitudinal and circumferential direction, L becomes less than $L_0$ resulting in negative longitudinal and circumferential strain. In contrast, radial thickening results in L becoming greater than $L_0$, thus radial strain is positive.

Myocardial strain is illustrated by strain curves, with time depicted on the x-axis and percent-strain on the y-axis. The LV is divided into six myocardial segments with corresponding, color-coded strain curves. Myocardial shortening during LV contraction is demonstrated by negative curves for longitudinal and circumferential strain, while radial strain is demonstrated by positive strain curves reflecting systolic thickening. Strain curves return to baseline at end-diastole (Fig. 3, 4, 5; Video 1).

Because myocardial segments do not always achieve peak myocardial deformation at the same time, especially in patients with electrical or mechanical dyssynchrony, the exact time of segmental strain measurement during the cardiac cycle affects the measured value. For example, end-systolic strain is strain measured precisely at end-systole, defined by time of aortic valve closure. This value may differ from peak systolic strain, which is a measurement of peak deformation at any point during systole (Table 1, Fig. 3). Global strain represents average strain for all myocardial segments and can be calculated in the longitudinal, circumferential and radial direction. When describing an alteration in strain, most adhere to the convention of using the absolute value to describe the change of strain (e.g. a change of −18% to −12% reflects a "decrease" in strain).

## Strain rate

SR is the temporal derivative of strain and is defined as change in strain per unit time and described in unit measurements of $sec^{-1}$. SR describes speed of myocardial deformation or the rate of shortening or lengthening of a myocardial segment. SR is defined as:

$$\mathrm{SR}=\Delta\varepsilon/\Delta\mathrm{t},$$

where ε = myocardial strain and t = time. Full assessment of myocardial deformation requires consideration of both strain (amount of deformation) and SR (speed of deformation). Strain and SR provide complementary information since patients with similar strain measurements may have different SR. For example, segmental strain in professional football players is similar to sedentary controls, but SR in mid-septal and mid-lateral walls is increased.[15] Furthermore, dobutamine infusion has minimal effect on strain but significantly increases SR in nonischemic myocardium.[16]

SR signals have more noise than strain; similar to strain, they are displayed with time on the x-axis and SR on the y-axis (Fig. 6). Similar to strain curves, systolic shortening in the longitudinal and circumferential directions produces negative SR, while radial thickening produces positive SR. Typically, SR peaks in mid-systole, then decelerates to zero at end-systole. A biphasic pattern occurs during isovolumic periods.[17] Average longitudinal systolic SR in subjects without cardiovascular disease measured by transthoracic echocardiography is (mean ± SD) −1.10 ± 0.16 $sec^{-1}$.[18]

SR diastolic curves consist of an early ($SR_E$) and late peak ($SR_A$), corresponding to early LV filing and atrial contraction. $SR_E$ reflects the time constant of LV relaxation and regional stiffness.[19] $SR_A$ represents passive LV "stretching" by propagation of pressure and flow caused by atrial systole.[20] Diastasis is represented by the relatively flat portion between these peaks when SR is near zero. Average $SR_E$ in healthy subjects is 1.55 ± 0.16 $sec^{-1}$.[18]

## Methods for measurement of myocardial strain and strain rate

Strain and SR were initially described with sonomicrometry, which involves implantation of ultrasonic crystals in the LV to assess myocardial fiber shortening and changes in ventricular dimensions.[21,22] There are two echocardiographic techniques/methods which have been

developed to assess LV deformation noninvasively, which include tissue Doppler imaging (TDI) and speckle-tracking echocardiography.

Measurements of strain using TDI are derived by integrating SR over time. Myocardial tissue velocities are measured at two points relative to the transducer.[12,14] SR is estimated from the spatial velocity gradient described as

$$\mathrm{SR}=(\mathrm{v}_a-\mathrm{v}_b)/d,$$

where $\mathrm{v}_a - \mathrm{v}_b$ represents the difference in myocardial velocities at points *a* and *b*, and *d* represents distance between these points.

Measurement of TDI strain requires an optimized 2D image and rapid frame rates to resolve regional velocities and calculate SR. Importantly, alignment of the Doppler beam with the myocardial region of interest is necessary, since an angle of incidence more than 20 degrees will result in inaccurate measurements. Strain is calculated from each sample volume and displayed in graphical format. TDI strain has been validated using sonomicrometry in animals[23,24] and magnetic resonance imaging (MRI) in humans.[25,26]

TDI strain has important limitations. As mentioned above, TDI strain is angle-dependent and can only accurately measure the component of motion parallel to the ultrasound beam direction. This limitation affects its use in the operating room because the transesophageal approach has limited ability to modify the incident beam angle. Thus a myocardial wall which curves inwards towards the apex or demonstrates a vector of motion which is poorly aligned with the ultrasound beam may result in underestimated myocardial velocities and strain (Fig. 7). Furthermore, TDI strain provides only the axial component of strain aligned with the ultrasound scan line; thus TDI strain measures only longitudinal deformation from long-axis views of the LV. From the transgastric short-axis window, it is possible to assess radial deformation of the anterior or inferior walls from the short-axis[6,27] and circumferential deformation in the septum and lateral wall. Importantly, myocardial deformation with TDI may be compromised by tethering or translation.

TDI strain is also limited by reverberation or dropout artifacts, which interfere with measurement of myocardial velocities and result in inaccurate strain or SR estimates. Furthermore, if the color scale is set too low during measurement of TDI strain, color velocity data can alias to the opposite direction. Poor tracking of the sample volume provides noisy data that are difficult to interpret, and inadvertent inclusion of velocity measurement from immobile tissue or artifact in the sample volume adversely affects calculations.[27] TDI strain has a relatively low signal-to-noise ratio, and requires considerable experience for correct interpretation.[28] Also, because the analysis includes operator-dependent functions, including the position of the sample volume, TDI strain is semiobjective. Because of these limitations, other methods to calculate myocardial strain have been developed. Speckle-tracking echocardiography is a newer, non-Doppler angle-independent technique for measurement of myocardial strain.

Speckle-tracking assesses myocardial movement and deformation by tracking “speckles” in echocardiographic images. A unique pattern or “fingerprint” of bright and dark pixels, or speckles, in standard B-mode (2D) echocardiographic images remains fairly consistent within a small region in the myocardium. These speckles, which are constructive and destructive interference patterns generated by reflected ultrasound from inhomogeneous myocardial tissue, are tracked from one frame to another throughout the cardiac cycle. A software algorithm extracts displacement, velocity, SR, and strain within the defined myocardial segment (Fig. 8).

Because displacement of the region of interest is measured relative to the previous frame rather than the ultrasound beam, speckle-tracking strain measurements are angle-independent. In contrast to TDI strain, which measures strain along the ultrasound beam, speckle-tracking strain calculates deformation in two axes and thus can measure strain simultaneously in the longitudinal and transverse direction from long-axis views, and radial and circumferential direction from short-axis views (Fig. 9). Speckle-tracking strain is less susceptible to tethering or translation artifacts: ischemic myocardial segments may demonstrate displacement and velocity due to tethering, but if deformation does not occur, regional strain and SR will be near zero, thus distinguishing active contraction from passive motion. Speckle-tracking strain and SR provide robust measurements of myocardial deformation with acceptable intraobserver and interobserver variability,[8] which correlates with sonomicrometry in dogs under changing loading conditions and regional ischemia,[29] and in humans measured by MRI tagging.[29]

Speckle-tracking echocardiography is limited by its dependence upon the quality of echocardiographic images, which affect the ability to track the speckle pattern and endocardial border. Inadequate tracking may occur because the complicated 3D motion of the heart causes out-of-plane motion, making it difficult to track speckles from image to image. Also, acoustic shadowing and reverberations interfere with frame-by-frame tracking which decrease accuracy of measurement.

Speckle-tracking uses lower frame rates (typically 50 to 90 frames/s) than TDI strain, which may result in movement of the speckle pattern outside the search area and poor tracking.[14] Furthermore, lower frame rates may compromise the ability to capture rapid events during the cardiac cycle. Thus SR measurements, which require high temporal resolution, may be less accurate with speckle-tracking than TDI.[30] Because strain analysis with speckle-tracking also involves operator-dependent functions, such as positioning of the region of interest and approval of myocardial tracking; quantification of global and regional measures using this technique are semiobjective. But despite these limitations, speckle-tracking provides a simpler, more reproducible, and angle-independent technique to estimate strain in the operating room and serves as the best option for assessing intraoperative regional myocardial function.

## Intraoperative deformation analysis

The following discussion describes intraoperative analysis of myocardial deformation using TDI and speckle-tracking methods with TEE. High-end echocardiographic machines, including the Vivid E9 (GE Healthcare Vingmed Ultrasound AS, Horten, Norway), which

uses Automated Function Imaging, and the IE33 (Philips Ultrasound, Andover, MA), which uses Cardiac Motion Quantification, have built-in capability of calculating strain using TDI and speckle-tracking methods allowing intraoperative myocardial deformation analysis.

**Measurement of strain with TDI—**Analysis of TDI myocardial strain requires excellent quality 2D echocardiographic images with optimal visualization of myocardial tissue and endocardial border. Artifacts which cause shadowing and reverberations that interfere with tracking should be minimized. TDI strain is angle-dependent, and thus adequate alignment of the ultrasound beam with the region of interest and the vector of myocardial motion is necessary to ensure accurate measurement. TEE midesophageal 4-chamber view may allow adequate beam alignment for measurement of longitudinal TDI strain in the inferoseptal and basal anterolateral wall. Narrowing the image sector of a single myocardial wall may improve beam alignment[11,12] and frame rate, and thus the analytical ability of Doppler deformation techniques. Radial strain may be measured in the inferior or anterior wall using a transgastric short-axis view.

TDI strain requires use of color tissue Doppler for image acquisition using a frame rate more than 100 frames/sec to resolve regional velocities and calculate SR. The velocity scale is adjusted to avoid aliasing. Three beats using color tissue Doppler with a clear electrocardiogram signal are stored in raw data format. Sample volumes are placed on the prerecorded echocardiographic clips in properly aligned basal-, mid-, or apical segments. Importantly, only areas where the vector of motion lies reasonably along the Doppler plane should be assessed. Furthermore, the position of a sample volume that is stationary will not track myocardial movement and thus the region of interest may not remain within the sampling area during the cardiac cycle. For this reason, some software programs allow manual frame-by-frame adjustment of the position of the sample volume to track the region of interest throughout the cardiac cycle. However, manual adjustment of the sample volume position is tedious and thus poorly suited for the intraoperative environment. After the sample volume is appropriately positioned, strain or SR mode is selected in the software analysis software, and the results are displayed. (Fig. 7)

**Measurement of Strain with Speckle-tracking Echocardiography—**A step-by-step process for intraoperative myocardial strain analysis is demonstrated in Table 2, Fig. 10 and Video 2. Analysis of myocardial deformation using speckle-tracking echocardiography requires optimal 2D echocardiographic images. Speckle-tracking strain is angle-independent; thus the ultrasound beam does not need to align with the direction of motion or region of interest. Collection of midesophageal long-axis, four-chamber, and two-chamber (between 60 and 90 degrees) echocardiographic clips with a similar heart rate (within 10 beats/min) is required for analysis. Shadowing from mitral calcification or a prosthetic mitral valve which obscures visualization of the myocardium and thus interferes with tracking of the speckles should be avoided. Images with poor endocardial border definition may also be susceptible to poor tracking (Video 3). Sometimes slight angle adjustment or anteflexion/retroflexion of the TEE probe may avoid artifacts and improve visualization and thus tracking of the myocardium.

An electrocardiogram with clearly defined P waves and QRS complexes is required for the accurate timing of the cardiac cycle. Closure of the aortic valve, which defines end-systole and thus the temporal relationship of deformation measures, can be determined by direct visualization from 2D echocardiographic images, spectral Doppler, or M-mode imaging of the aortic valve. If aortic valve closure is difficult to identify, some analysis programs automatically identify end-systole by calculating the average time to peak strain within each myocardial segment.

The technique for longitudinal deformation analysis is preset in some vendor-specific software, where strain analysis begins with placement of markers in a still frame of the midesophageal long-axis echocardiographic image. These markers are placed on the endocardial border adjacent to the mitral and aortic valve annulus, with another marker at the LV apex. The position of these markers is processed creating a colored pattern overlaying the LV in the “region of interest” which “tracks” myocardial motion throughout the cardiac cycle. The user visually reviews the tracking of the myocardium and, if acceptable, confirms that this pattern follows myocardial contraction accurately. If the tracking pattern does not adequately follow the endocardial border (Video 3), endocardial markers may need repositioning. If a segment of the LV consistently tracks poorly as described above, an untrackable segment is best excluded to avoid contamination of global calculations. The user can exclude segments simply by not confirming acceptable tracking. Most vendor-specific software will still calculate global strain if one of six segments is not tracked.

Once users confirm acceptable tracking of myocardium, the analysis program calculates frame-to-frame displacement of the speckle pattern throughout the cardiac cycle and displays segmental and global longitudinal strain. After strain analysis is completed in the three chosen views, some software programs incorporate deformation parameters into a “bull’s eye” view to provide an overall picture of global and regional LV function using numerical and color-coded parameters (Fig. 10, lower right panel). Most strain analysis software, however, is oriented toward the transthoracic echocardiography perspective.

For research purposes, a more comprehensive analysis can be performed off-line using advanced research software programs such as EchoPAC (GE Healthcare) or QLab (Philips Ultrasound), which provide detailed information about strain parameters and substantial opportunity to adjust preferences and data collection procedures. Another software package called Velocity Vector Imaging (VVI, Syngo Velocity Vector Imaging technology, Siemens Medical Solutions, Mountain View, California) uses a novel method of feature-tracking that incorporates speckle-tracking with tracking of the endocardial contour; it can be used with any ultrasound image in standard DICOM format and can thus be used on recordings from various vendors. Additional software options are detailed in Table 3.

## Interpretation of “normal” strain values

Normal reference values for longitudinal, circumferential, and radial strain are shown in Table 4. Importantly, these “normal” reference values were measured by transthoracic echocardiography in healthy subjects who were awake and breathing spontaneously.[18,31] Thus these values may vary from patients who are anesthetized and whose lungs are

mechanically ventilated and evaluated with TEE. Certainly, the choice of transthoracic versus transesophageal approach may affect strain measures.[32,33] And since general anesthesia affects myocardial function,[34,35] strain measured in anesthetized patients may differ from norm reference values. Furthermore, intraoperative events such as pericardial opening impact ventricular function and hemodynamic measures[36,37] and may affect intraoperative strain. For these reasons, strain measured in the operating room may differ from published normal reference values. Unfortunately, reference values specific for anesthetized patients measured by TEE are unavailable. Thus, current options are limited to reference values acquired from transthoracic echocardiography.

Technical factors affect strain measures, including whether Doppler versus non-Doppler methods or which data postprocessing techniques or software analysis packages are used.[38] Software options for strain analysis and a comparison of these software options are shown in Tables 3 and 5. Interestingly, despite presumed differences with software analysis and techniques, one recent meta-analysis reported that strain measurements were not affected by the choice of analysis package, although there may have been insufficient heterogeneity of echocardiographic equipment to thoroughly evaluate this variable.[39] Importantly, when strain is measured with TEE using the same analysis software under similar conditions, results are highly reproducible in the operating room.[33] A comparison of myocardial function and strain calculations in patients with normal, moderately decreased, and severely decreased myocardial function is shown in Video 4.

## The effect of loading conditions and heart rate on strain and SR

Because myocardial deformation reflects the interaction between myocardial loading conditions and contractility, changes in loading conditions influence myocardial deformation. SR is highly correlated with LV end-systolic pressure-volume relationship and the rate of rise of LV pressure (dP/dt) and thus is a robust noninvasive measure of LV contractility.[40–43] However, dP/dt and other measures of myocardial contractility are subject to changes in contractile state, preload, and afterload,[44] thus strain and SR may also be affected.

Changes in loading conditions affect all components of myocardial deformation. In animals, longitudinal strain and SR were reduced when afterload was increased, whereas increased preload increased strain and SR by the Frank Starling mechanism.[45] Radial and circumferential strain are sensitive to changes in afterload, while SR is a more robust measure of contractility, because it is less influenced by alterations in preload and afterload.[46] Strain is inversely related to heart rate in some[42] but not all animal models.[47] Heart rate has less effect on Doppler SR than strain.[42] Because acute changes in load occur during surgery, serial echocardiographic examinations performed intraoperatively, should take changes in heart rate, preload, and afterload into consideration.

## Measures of right ventricular deformation

Deformation is useful for assessment of right ventricular (RV) function. Because afterload is lower and compliance is higher in the RV, RV velocities are consistently greater than the LV. Since longitudinal shortening provides the largest contribution to RV performance, RV

function can be largely assessed using longitudinal strain and SR. Global RV strain and SR in healthy subjects are −29.5 ± 5.5% and −2.1 ± 0.4 $sec^{-1}$.[48] An RV ejection fraction of ≥ 50% is typically accompanied by systolic strain at the basal RV free wall of −25%, and a SR of −4 $sec^{-1}$ measured with TDI strain.[49]

Subclinical RV dysfunction can be identified by strain analysis. After mitral valve surgery, for example, reduced RV longitudinal strain is evident in patients with normal 3D RV ejection fractions.[50] Furthermore, asymptomatic patients with diabetes demonstrate subclinical RV dysfunction with reduced RV systolic strain, SR, and early diastolic SR.[51] RV strain and SR abnormalities are also seen with amyloidosis, congenital heart disease, and arrhythmogenic RV cardiomyopathy. In patients with chronic heart failure, RV strain less than −21% is associated with acute heart failure and death.[48] Pulmonary hypertension significantly reduces RV strain, while also impacting LV strain and torsion.[52]

## Twist and Torsion

Speckle-tracking provides a noninvasive alternative to sonomicrometry and tagged MRI for evaluation of the complex 3D contractile motion of the LV, dictated by the spiral structure of the myocardial fibers. The subendocardium consists of myocardial fibers oriented in a right-handed helix evolving gradually into a left-handed helix in the subepicardium.[10–12] Subendocardial fibers are nearly longitudinally oriented (an angle of approximately 80 degrees with respect to the circumferential direction of the heart); the mid-myocardial fibers are parallel to the circumferential direction (at approximately 0 degrees), and subepicardial fibers are at −60 degrees.[10–12] This ventricular structure enables a twisting or “wringing” motion during systole (Fig. 11).

During isovolumic contraction, the apex briefly rotates in a clockwise direction, but quickly reverses into a counterclockwise direction during ejection when viewed from the apex. Concurrently, the base rotates in a clockwise direction around the LV long-axis.[53] This twisting motion of the LV causes thickening and longitudinal shortening of the myocardium, while concurrent circumferential shortening causes LV ejection. Untwist, the subsequent recoil of twist, occurs during diastole when restoring forces are released causing diastolic suction and facilitation of early LV filling. Most untwisting occurs during isovolumic relaxation and is completed during early diastole.[54] The terms, LV rotation, twist, and torsion, describe the complex 3D myocardial motion and are sometimes used interchangeably. For the purpose of this discussion, LV rotation measures degrees of rotation viewed from the apex,[53] and LV twist is calculated as rotation of the apex relative to the base or, in other words, the absolute apex-to-base difference in rotation measured in degrees.[55] (Table 1) Torsion refers to the apex-to-base gradient in the rotation angle of the LV long axis: the apex-to-base twist angle is divided by the distance between measured locations of the base and apex and is thus calculated in degrees per centimeter.[11,12] Both TDI [56] and speckle-tracking echocardiography[57] allow calculation of twist and torsion from LV short-axis views.

Normal value for twist in healthy volunteers is 7.7 ± 3.5 degrees. These values increase with age, likely because of less opposition to apical rotation.[11,12] Thus LV twist is higher in healthy subjects older than 60 years of age compared with those younger than 40 years old

(10.8 ± 4.9 vs. 6.7 ± 2.9 degrees, respectively).[55] Apical wall motion abnormalities, however, significantly impair LV twist. Delay of LV untwisting may partially explain diastolic dysfunction in patients with LV hypertrophy[54,58] and age-related diastolic abnormalities.[55] Torsion, in contrast, is normally about 3 degrees and does not change significantly with age.[59] LV twist and untwist have a profound impact on LV systolic and diastolic mechanics and may allow detection of systolic and diastolic abnormalities in surgical patients; however, perioperative application of this technique requires further investigation.

### Clinical application of strain

Myocardial deformation analysis objectively quantifies alterations in LV function; thus subtle changes in myocardial function during the perioperative period can be detected with strain analysis. Myocardial deformation analysis can differentiate between regional dysfunction, such as coronary artery occlusion, and global myocardial dysfunction, such as ischemia-reperfusion injury. Because systolic wall motion abnormalities occur within seconds of coronary occlusion,[60] alterations in deformation appear quickly after onset of ischemia in affected myocardial segments. Thus new regional wall motion abnormalities caused by an acute coronary bypass graft occlusion can be identified by an acute reduction in strain in the affected coronary artery territory. In addition, strain measured with speckle-tracking echocardiography can distinguish between true myocardial contraction and passive myocardial segmental motion in patients suspected of having a myocardial infarction. An example of an acute transmural myocardial infarction causing severe hypokinesis and akinesia in affected myocardial segments is shown in Fig. 12.

In contrast to regional alterations in strain caused by coronary artery occlusion, ischemia and reperfusion injury or myocardial stunning demonstrate global alterations in myocardial deformation, which involve reductions in myocardial strain in multiple myocardial segments without directly corresponding to a specific coronary artery territory. This distinction between regional and global alterations in myocardial deformation is important, because regional ischemia may prompt antiischemic or thrombolytic therapy or possibly revascularization, whereas global myocardial dysfunction occurring with hypotension or hemodynamic instability, suggests a need for generalized hemodynamic support. Strain measurements may thus guide anesthetic management and determine therapeutic intervention.

## Early detection of myocardial disease

Myocardial deformation imaging can detect subtle myocardial pathology and small decrements in myocardial performance before overt disease is apparent. In the following sections, alterations in LV mechanics which characterize various cardiac pathologies are discussed (Table 6).

### Myocardial deformation in ischemic heart disease

Patients with coronary artery disease demonstrate abnormal myocardial deformation. Attenuated longitudinal strain measurements provide an early indication of subendocardial

ischemia,[61–63] though nonischemic myocardial regions may compensate for impaired systolic function with increased shortening.[60,64] In patients with coronary artery disease, longitudinal segmental strain cutoffs of −14.1% and −6.65% detected ischemic and infarcted myocardial segments, respectively.[65] Patients with recent anterior wall myocardial infarction demonstrate reduced radial and longitudinal strain, while greater reduction in circumferential strain is seen if LVEF is reduced.[65,66]

Deformation analysis may demonstrate distinct findings suggestive of asynchronous myocardial contraction during ischemia. For example, postsystolic shortening, characterized by the occurrence of peak strain after end-systole, is highly sensitive, although nonspecific, for ischemia (Fig. 13).[16,60,67–70] Prestretch, demonstrated by early systolic lengthening before later systolic shortening, may occur with regional ischemia[16] though prestretch may be a normal finding related to slight conduction delays.[11,12] Since visual recognition of asynchronous myocardial contraction is unreliable,[71] examination of strain curves may permit early detection of asynchronicity in the operating room.

Ischemic heart disease affects other variables of myocardial deformation. For example, patients with myocardial ischemia have reduced longitudinal and circumferential SR at rest and during dobutamine stress echocardiography.[65,72] Peak twist and untwist decreases after anterior wall myocardial infarction corresponding to the severity of LV dysfunction.[66] When LV deformation and twist mechanics are significantly affected by ischemia, myocardial performance worsens.

Because a delay in LV relaxation often precedes systolic wall motion abnormalities,[73] indices of diastolic function may provide earlier indications of ischemia.[64] For example, early diastolic SR was significantly reduced in ischemic myocardial segments.[62] And substantial delays in early LV relaxation during exercise in patients with stable effort angina, measured as a radial strain diastolic index, provided a sensitive method for detection of myocardial ischemia.[74]

### Myocardial deformation in valvular disease

Patients with valvular disease experience ventricular remodeling as a consequence of chronic volume or pressure overload where structural and histopathologic changes to the myocardium lead to a progressive decline in LV function. If prolonged, LV remodeling becomes irreversible. Altered strain patterns can identify subclinical decrements in LV function, which may improve timing for surgical intervention before irreversible myocardial dysfunction occurs.[75,76]

LVEF is often preserved or increased in patients with mitral regurgitation because of compensatory changes in preload and afterload. However, despite normal LVEF, asymptomatic patients with mitral regurgitation often demonstrate reduced longitudinal and radial strain.[77] Longitudinal SR may be more attenuated than circumferential or radial SR.[78] Furthermore, LV untwisting is delayed in patients with mitral regurgitation and may provide early signs of LV dysfunction.[79]

Strain analysis allows detection of subclinical LV dysfunction,[80] which may predict postoperative outcomes. In patients with severe degenerative mitral regurgitation, preoperative global longitudinal strain worse than −18% was associated with abnormal postoperative LV function.[75] Likewise, reduced preoperative longitudinal strain predicted a 10% or greater reduction in postoperative LVEF.[77] Abnormal longitudinal and radial SR identified patients at risk for irreversible myocardial damage.[81] Moreover, a recent study found that impaired longitudinal strain worse than −19.9% predicted long-term LV dysfunction after mitral valve repair.[82] Thus, preoperative measures of deformation predict postoperative myocardial function in patients with mitral regurgitation.

Aortic regurgitation induces LV remodeling and a significant increase in LV end-diastolic volume, which can mask onset of clinical LV dysfunction. However, strain analysis detects reduced longitudinal strain in young athletes with bicuspid aortic valves and mild aortic insufficiency,[83] though others reported normal mechanics in patients with aortic regurgitation.[84] Outer circumferential and radial strain may actually increase in early stages to preserve LVEF and compensate for reduced inner circumferential and radial strain;[85] but in later stages of disease, radial and longitudinal function decline.[86] Longitudinal and radial peak systolic SR are reduced with advanced aortic regurgitation and are inversely correlated with LV end-systolic and end-diastolic volumes.[86]

Preoperative detection of abnormal strain in patients with aortic regurgitation may improve timing of surgical intervention resulting in improved myocardial function and postoperative outcomes.[76] Reduced preoperative systolic myocardial strain increases risk of heart failure, dilated LV, and impaired LV function after aortic valve replacement surgery.[87] Decreased preoperative radial SR less than 1.82 $sec^{-1}$ was highly sensitive and specific for detecting postoperative LVEF less than 50%.[88] Thus, detection of abnormal LV mechanics may improve preoperative risk stratification and provide an earlier opportunity for clinical intervention in attempts to improve postoperative outcomes.

Aortic stenosis results in progressive LV hypertrophy in response to chronically increased afterload, but LVEF is preserved until late stages of disease. LV systolic longitudinal strain and SR may nonetheless be attenuated early because of interstitial fibrosis, and the presence of abnormal strain may predict worse outcomes. Patients with asymptomatic aortic stenosis demonstrate impaired global longitudinal strain, especially in basal segments, and, basal longitudinal strain worse than −13% increased risk of rehospitalization, aortic valve surgery, and death.[89] With progression of aortic stenosis and interstitial myocardial fibrosis, deformation analysis demonstrates reduced longitudinal, circumferential, and radial strain, with reduced SR.[90,91] Twist mechanics in patients with aortic stenosis are also affected resulting in increased apical rotation and greater LV torsion, perhaps in compensation for increased intracavitary pressure.[92] Fortunately, strain improves in all dimensions after aortic valve replacement.[90,93]

### Hypertensive Heart Disease and other Cardiomyopathies

Myocardial deformation is abnormal in hypertensive heart disease because of chronically increased afterload, LV hypertrophy, and progressive myocardial fibrosis. Longitudinal strain is reduced with hypertensive heart disease,[94–96] which correlates with markers of

myocardial collagen turnover and interstitial fibrosis.[97] Circumferential strain, however, remains normal or even increases in early stages.[94–96] However, when concentric LV hypertrophy develops, strain and SR decrease in all directions.[96,98,99] Diastolic dysfunction is evident with LV hypertrophy by reduced early diastolic peak relaxation rate.[94] Twist or torsion may decrease, but occasionally experiences a compensatory increase.[95,97,98] Thus, subclinical abnormalities are evident with myocardial deformation analysis.

Hypertrophic cardiomyopathy is characterized by myocardial fiber disarray and eventual LV systolic and diastolic dysfunction. Measurement of myocardial deformation in patients with early disease detects global subclinical systolic dysfunction with reduced longitudinal, radial, and circumferential strain corresponding to the degree of ventricular fibrosis[100,101] and associated with functional status.[102] However, paradoxical systolic lengthening sometimes occurs.[103] Longitudinal systolic and diastolic SR is also reduced compared to subjects without disease.[104] In contrast, overall LV twist remains near normal, although subtle rotation abnormalities may be present.[102] LV untwisting is slowed and the increase in LV untwisting rate associated with exercise is blunted.[54]

Dilated cardiomyopathy demonstrates diminished systolic strain and SR in all directions.[94,105,106] Interestingly, global longitudinal strain is a better predictor of arrhythmic events than LVEF in cardiomyopathy patients.[107] Torsional and diastolic deformation variables including peak relaxation rate are also reduced,[94,105] and LV rotation is abnormal.[105]

### Diastolic and systolic heart failure syndromes

Patients with heart failure and preserved ejection fraction, termed “diastolic heart failure,” have abnormalities of both systolic and diastolic function at rest which worsen with exercise as measured by stress echocardiography.[108] Despite the fact that patients with early diastolic heart failure may maintain normal LVEF, they typically have attenuated longitudinal systolic strain compensated by preserved LV twist and circumferential strain.[109] A decrease in circumferential strain reflects more advanced disease and is associated with worse outcomes. Indeed, abnormal global circumferential strain predicted re-hospitalization and cardiac death.[9] Systolic heart failure demonstrates reduced circumferential strain and LV twist[109] consistent with late impairment of LV function.[110] Abnormal longitudinal strain predicts mortality in patients with heart failure more accurately than LVEF,[7] and peak LV twist and untwisting rate are decreased in patients with heart failure.[111]

## The future of intraoperative echocardiographic strain assessment

The use of myocardial deformation analysis has clinically important perioperative value. Because TDI strain is compromised by its angle-dependence, a significant limitation especially when using the transesophageal approach, strain measured with speckle-tracking echocardiography has greater potential for intraoperative use. Strain measured with speckle-tracking echocardiography is angle-independent and can measure two axes simultaneously. Though some software analyses programs loaded on the echocardiographic workstation currently provide only assessment of longitudinal deformation, more options for measurement of radial and circumferential strain may become available in the future.

Speckle-tracking echocardiography is currently limited by the lack of standardization among vendors.[112–114] Fortunately, there is currently a joint effort among the American Society of Echocardiography, European Association of Cardiovascular Imaging, and industry to standardize methodology for speckle-tracking echocardiography. Standardization would allow clinicians to comparably interpret results generated by equipment from various vendors.

Three-dimensional speckle-tracking technology has been introduced for transthoracic echocardiography,[115] but is not yet available for TEE. This technology remains limited by a low frame rate and poor temporal resolution. It is likely, though, that 3D speckle-tracking will bypass limitations of out-of-plane motion inherent in 2D imaging. Especially at acceptable frame rates of 18 or 25 frames/sec, 3D strain analysis appears to adequately estimate myocardial strain.[116] Three-dimensional speckle tracking may provide an opportunity to evaluate motion of all myocardial segments in a single analysis step, thereby significantly reducing analysis time.[117]

In summary, measurement of myocardial deformation provides important quantitative information on global and regional myocardial function. It is thus likely that echocardiographic evaluation of strain and SR will increasingly be incorporated into clinical practice. That said, the technique is relatively new and more research will be required to identify the diagnostic accuracy of different strain and SR variables and their reproducibility in various disease states. Future studies will also determine the extent to which strain and SR measurements can enhance patient management and improve postoperative outcomes.

## Supplementary Material

Refer to Web version on PubMed Central for supplementary material.

## Acknowledgments

**Funding:** supported by NIH HL093065 (Dr. Duncan) and the Departments of Cardiothoracic Anesthesia, Outcomes Research, and Cardiovascular Medicine Cleveland Clinic, Cleveland, OH.

## References

1. Ranucci M, Castelvecchio S, Menicanti L, Frigiola A, Pelissero G. Risk of Assessing Mortality Risk in Elective Cardiac Operations: age, Creatinine, Ejection Fraction, and the Law of Parsimony. Circulation. 2009; 119:3053–61. [PubMed: 19506110]
2. Sprung J, Abdelmalak B, Gottlieb A, Mayhew C, Hammel J, Levy PJ, O'Hara P, Hertzer NR. Analysis of risk factors for myocardial infarction and cardiac mortality after major vascular surgery. Anesthesiology. 2000; 93:129–40. [PubMed: 10861156]
3. Rohde LE, Polanczyk CA, Goldman L, Cook EF, Lee RT, Lee TH. Usefulness of transthoracic echocardiography as a tool for risk stratification of patients undergoing major noncardiac surgery. Am J Cardiol. 2001; 87:505–9. [PubMed: 11230829]
4. Flu WJ, van Kuijk JP, Hoeks SE, Kuiper R, Schouten O, Goei D, Elhendy A, Verhagen HJ, Thomson IR, Bax JJ, Fleisher LA, Poldermans D. Prognostic Implications of Asymptomatic Left Ventricular Dysfunction in Patients Undergoing Vascular Surgery. Anesthesiology. 2010; 112:1316–24. [PubMed: 20502115]

5. Bergquist BD, Leung JM, Bellows WH. Transesophageal echocardiography in myocardial revascularization: I. Accuracy of intraoperative real-time interpretation. Anesth Analg. 1996; 82:1132–8. [PubMed: 8638780]
6. Skubas NJ. Two-dimensional, non-Doppler strain imaging during anesthesia and cardiac surgery. Echocardiography. 2009; 26:345–53. [PubMed: 19291020]
7. Mignot A, Donal E, Zaroui A, Reant P, Salem A, Hamon C, Monzy S, Roudaut R, Habib G, Lafitte S. Global longitudinal strain as a major predictor of cardiac events in patients with depressed left ventricular function: a multicenter study. J Am Soc Echocardiogr. 2010; 23:1019–24. [PubMed: 20810243]
8. Becker M, Bilke E, Kühl H, Katoh M, Kramann R, Franke A, Bücker A, Hanrath P, Hoffmann R. Analysis of myocardial deformation based on pixel tracking in two dimensional echocardiographic images enables quantitative assessment of regional left ventricular function. Heart. 2006; 92:1102–8. [PubMed: 16387826]
9. Cho GY, Marwick TH, Kim HS, Kim MK, Hong KS, Oh DJ. Global 2-dimensional strain as a new prognosticator in patients with heart failure. J Am Coll Cardiol. 2009; 54:618–24. [PubMed: 19660692]
10. Skubas N. Intraoperative Doppler tissue imaging is a valuable addition to cardiac anesthesiologists' armamentarium: a core review. Anesth Analg. 2009; 108:48–66. [PubMed: 19095830]
11. Mor-Avi V, Lang RM, Badano LP, Belohlavek M, Cardim NM, Derumeaux G, Galderisi M, Marwick T, Nagueh SF, Sengupta PP, Sicari R, Smiseth OA, Smulevitz B, Takeuchi M, Thomas JD, Vannan M, Voigt JU, Zamorano JL. Current and evolving echocardiographic techniques for the quantitative evaluation of cardiac mechanics: ASE/EAE consensus statement on methodology and indications endorsed by the Japanese Society of Echocardiography. Eur J Echocardiogr. 2011; 12:167–205. [PubMed: 21385887]
12. Mor-Avi V, Lang RM, Badano LP, Belohlavek M, Cardim NM, Derumeaux G, Galderisi M, Marwick T, Nagueh SF, Sengupta PP, Sicari R, Smiseth OA, Smulevitz B, Takeuchi M, Thomas JD, Vannan M, Voigt JU, Zamorano JL. Current and evolving echocardiographic techniques for the quantitative evaluation of cardiac mechanics: ASE/EAE consensus statement on methodology and indications endorsed by the Japanese Society of Echocardiography. J Am Soc Echocardiogr. 2011; 24:277–313. [PubMed: 21338865]
13. Pavlopoulos H, Nihoyannopoulos P. Strain and strain rate deformation parameters: from tissue Doppler to 2D speckle tracking. Int J Cardiovasc Imaging. 2008; 24:479–91. [PubMed: 18074240]
14. Teske AJ, De Boeck BW, Melman PG, Sieswerda GT, Doevendans PA, Cramer MJ. Echocardiographic quantification of myocardial function using tissue deformation imaging, a guide to image acquisition and analysis using tissue Doppler and speckle tracking. Cardiovasc Ultrasound. 2007; 5:27. [PubMed: 17760964]
15. Tümüklü MM, Etikan I, Cinar CS. Left ventricular function in professional football players evaluated by tissue Doppler imaging and strain imaging. Int J Cardiovasc Imaging. 2008; 24:25–35. [PubMed: 17410479]
16. Voigt JU, Exner B, Schmiedehausen K, Huchzermeyer C, Reulbach U, Nixdorff U, Platsch G, Kuwert T, Daniel WG, Flachskampf FA. Strain-Rate Imaging During Dobutamine Stress Echocardiography Provides Objective Evidence of Inducible Ischemia. Circulation. 2003; 107:2120–6. [PubMed: 12682001]
17. Marcucci C, Lauer R, Mahajan A. New echocardiographic techniques for evaluating left ventricular myocardial function. Semin Cardiothorac Vasc Anesth. 2008; 12:228–47. [PubMed: 19033270]
18. Marwick TH, Leano RL, Brown J, Sun JP, Hoffmann R, Lysyansky P, Becker M, Thomas JD. Myocardial strain measurement with 2-dimensional speckle-tracking echocardiography: definition of normal range. JACC Cardiovasc Imaging. 2009; 2:80–4. [PubMed: 19356538]
19. Park TH, Nagueh SF, Khoury DS, Kopelen HA, Akrivakis S, Nasser K, Ren G, Frangogiannis NG. Impact of myocardial structure and function postinfarction on diastolic strain measurements: implications for assessment of myocardial viability. Am J Physiol Heart Circ Physiol. 2006; 290:H724–31. [PubMed: 16183729]

20. Stoylen A, Slordahl S, Skjelvan GK, Heimdal A, Skjaerpe T. Strain rate imaging in normal and reduced diastolic function: comparison with pulsed Doppler tissue imaging of the mitral annulus. J Am Soc Echocardiogr. 2001; 14:264–74. [PubMed: 11287889]
21. Rushmer RF, Franklin DL, Ellis RM. Left Ventricular Dimensions Recorded by Sonocardiometry. Circ Res. 1956; 4:684–8. [PubMed: 13365076]
22. Leraand S, Kiil F. Local Dimensional Changes of the Myocardium Measured by Ultrasonic Technique. Scand J Clin Lab Invest. 1969; 24:361–71. [PubMed: 5375743]
23. Urheim S, Edvardsen T, Torp H, Angelsen B, Smiseth OA. Myocardial strain by Doppler Echocardiography: validation of a new method to quantify regional myocardial function. Circulation. 2000; 102:1158–64. [PubMed: 10973846]
24. Skulstad H, Urheim S, Edvardsen T, Andersen K, Lyseggen E, Vartdal T, Ihlen H, Smiseth OA. Grading of Myocardial Dysfunction by Tissue Doppler Echocardiography. J Am Coll Cardiol. 2006; 47:1672–82. [PubMed: 16631008]
25. Edvardsen T, Gerber BL, Garot J, Bluemke DA, Lima JA, Smiseth OA. Quantitative assessment of intrinsic regional myocardial deformation by Doppler strain rate echocardiography in humans: validation against three-dimensional tagged magnetic resonance imaging. Circulation. 2002; 106:50–6. [PubMed: 12093769]
26. Herbots L, Maes F, D'hooge J, Claus P, Dymarkowski S, Mertens P, Mortelmans L, Bijnens B, Bogaert J, Rademakers FE, Sutherland GR. Quantifying myocardial deformation throughout the cardiac cycle: a comparison of ultrasound strain rate, grey-scale M-mode and magnetic resonance imaging. Ultrasound Med Biol. 2004; 30:591–8. [PubMed: 15183223]
27. Tousignant C. CON: Intraoperative Doppler Tissue Imaging Is a Valuable Addition to Cardiac Anesthesiologists' Armamentarium. Anesth Analg. 2009; 108:41–7. [PubMed: 19095829]
28. Marwick TH. Measurement of strain and strain rate by echocardiography: ready for prime time? J Am Coll Cardiol. 2006; 47:1313–27. [PubMed: 16580516]
29. Amundsen BH, Helle-Valle T, Edvardsen T, Torp H, Crosby J, Lyseggen E, Stoylen A, Ihlen H, Lima JA, Smiseth OA, Slordahl SA. Noninvasive myocardial strain measurement by speckle tracking echocardiography: validation against sonomicrometry and tagged magnetic resonance imaging. J Am Coll Cardiol. 2006; 47:789–93. [PubMed: 16487846]
30. Abraham TP, Pinheiro AC. Speckle-derived Strain: A Better Tool for Quantification of Stress Echocardiography? J Am Coll Cardiol. 2008; 51:158–60. [PubMed: 18191741]
31. Dalen H, Thorstensen A, Aase SA, Ingul CB, Torp H, Vatten LJ, Stoylen A. Segmental and global longitudinal strain and strain rate based on echocardiography of 1266 healthy individuals: the HUNT study in Norway. Eur J Echocardiogr. 2010; 11:176–83. [PubMed: 19946115]
32. Tousignant CP, Bowry R, Levesque S, Denault AY. Regional Differences in Color Tissue Doppler-Derived Measures of Longitudinal Right Ventricular Function Using Transesophageal and Transthoracic Echocardiography. J Cardiothorac Vasc Anesth. 2008; 22:400–5. [PubMed: 18503928]
33. Marcucci CE, Samad Z, Rivera J, Adams DB, Philips-Bute BG, Mahajan A, Douglas PS, Aronson S, Mackensen GB, Podgoreanu MV, Mathew JP, Swaminathan M. A comparative evaluation of transesophageal and transthoracic echocardiography for measurement of left ventricular systolic strain using speckle tracking. J Cardiothorac Vasc Anesth. 2012; 26:17–25. [PubMed: 21835637]
34. Vatner SF, Braunwald E. Cardiovascular control mechanisms in the conscious state. N Engl J Med. 1975; 293:970–6. [PubMed: 1101063]
35. Merin RG. Are the myocardial functional and metabolic effects of isoflurane really different from those of halothane and enflurane? Anesthesiology. 1981; 55:398–408. [PubMed: 7294375]
36. Chang S, Kim HK, Kim YJ, Cho GY, Oh S, Sohn DW. Role of pericardium in the maintenance of left ventricular twist. Heart. 2010; 96:785–90. [PubMed: 20448130]
37. Angelini GD, Fraser AG, Koning MM, Smyllie JH, Hop WC, Sutherland GR, Verdouw PD. Adverse hemodynamic effects and echocardiographic consequences of pericardial closure soon after sternotomy and pericardiotomy. Circulation. 1990; 82(IV):397–406.
38. Marwick TH. Will standardization make strain a standard measurement? J Am Soc Echocardiogr. 2012; 25:1204–6. [PubMed: 23089621]

39. Yingchoncharoen T, Agarwal S, Popovic ZB, Marwick TH. Normal ranges of left ventricular strain: a meta-analysis. J Am Soc Echocardiogr. 2013; 26:185–91. [PubMed: 23218891]
40. Greenberg NL, Firstenberg MS, Castro PL, Main M, Travaglini A, Odabashian JA, Drinko JK, Rodriguez LL, Thomas JD, Garcia MJ. Doppler-derived myocardial systolic strain rate is a strong index of left ventricular contractility. Circulation. 2002; 105:99–105. [PubMed: 11772883]
41. Jamal F, Strotmann J, Weidemann F, Kukulski T, D'hooge J, Bijnens B, Van de Werf F, De Scheerder I, Sutherland GR. Noninvasive quantification of the contractile reserve of stunned myocardium by ultrasonic strain rate and strain. Circulation. 2001; 104:1059–65. [PubMed: 11524402]
42. Weidemann F, Jamal F, Kowalski M, Kukulski T, D'Hooge J, Bijnens B, Hatle L, De Scheerder I, Sutherland GR. Can strain rate and strain quantify changes in regional systolic function during dobutamine infusion, B-blockade, and atrial pacing--implications for quantitative stress echocardiography. J Am Soc Echocardiogr. 2002; 15:416–24. [PubMed: 12019424]
43. Weidemann F, Jamal F, Sutherland GR, Claus P, Kowalski M, Hatle L, De Scheerder I, Bijnens B, Rademakers FE. Myocardial function defined by strain rate and strain during alterations in inotropic states and heart rate. Am J Physiol Heart Circ Physiol. 2002; 283:H792–9. [PubMed: 12124229]
44. Kass DA, Maughan WL, Guo ZM, Kono A, Sunagawa K, Sagawa K. Comparative influence of load versus inotropic states on indexes of ventricular contractility: experimental and theoretical analysis based on pressure-volume relationships. Circulation. 1987; 76:1422–36. [PubMed: 3454658]
45. Rosner A, Bijnens B, Hansen M, How OJ, Aarsaether E, Muller S, Sutherland GR, Myrmel T. Left ventricular size determines tissue Doppler-derived longitudinal strain and strain rate. Eur J Echocardiogr. 2009; 10:271–7. [PubMed: 18827033]
46. Ferferieva V, Van den Bergh A, Claus P, Jasaityte R, Veulemans P, Pellens M, La Gerche A, Rademakers F, Herijgers P, D'hooge J. The relative value of strain and strain rate for defining intrinsic myocardial function. Am J Physiol Heart Circ Physiol. 2012; 302:H188–95. [PubMed: 22081696]
47. Weytjens C, D'hooge J, Droogmans S, Van den Bergh A, Cosyns B, Lahoutte T, Herijgers P, Van Camp G. Influence of heart rate reduction on Doppler myocardial imaging parameters in a small animal model. Ultrasound Med Biol. 2009; 35:30–5. [PubMed: 18834657]
48. Guendouz S, Rappeneau S, Nahum J, Dubois-Rande JL, Gueret P, Monin JL, Lim P, Adnot S, Hittinger L, Damy T. Prognostic significance and normal values of 2D strain to assess right ventricular systolic function in chronic heart failure. Circ J. 2012; 76:127–36. [PubMed: 22033348]
49. Vitarelli A, Conde Y, Cimino E, Stellato S, D'Orazio S, D'Angeli I, Nguyen BL, Padella V, Caranci F, Petroianni A, D'Antoni L, Terzano C. Assessment of right ventricular function by strain rate imaging in chronic obstructive pulmonary disease. Eur Respir J. 2006; 27:268–75. [PubMed: 16452579]
50. Maffessanti F, Gripari P, Tamborini G, Muratori M, Fusini L, Alamanni F, Zanobini M, Fiorentini C, Caiani EG, Pepi M. Evaluation of right ventricular systolic function after mitral valve repair: a two-dimensional Doppler, speckle-tracking, and three-dimensional echocardiographic study. J Am Soc Echocardiogr. 2012; 25:701–8. [PubMed: 22542273]
51. Kosmala W, Przewlocka-Kosmala M, Mazurek W. Subclinical right ventricular dysfunction in diabetes mellitus—an ultrasonic strain/strain rate study. Diabet Med. 2007; 24:656–63. [PubMed: 17367309]
52. Puwanant S, Park M, Popovic ZB, Tang WH, Farha S, George D, Sharp J, Puntawangkoon J, Loyd JE, Erzurum SC, Thomas JD. Ventricular geometry, strain, and rotational mechanics in pulmonary hypertension. Circulation. 2010; 121:259–66. [PubMed: 20048214]
53. Sengupta PP, Tajik AJ, Chandrasekaran K, Khandheria BK. Twist Mechanics of the Left Ventricle. JACC: Cardiovasc Imaging. 2008; 1:366–76. [PubMed: 19356451]
54. Notomi Y, Martin-Miklovic MG, Oryszak SJ, Shiota T, Deserranno D, Popovic ZB, Garcia MJ, Greenberg NL, Thomas JD. Enhanced ventricular untwisting during exercise: a mechanistic manifestation of elastic recoil described by Doppler tissue imaging. Circulation. 2006; 113:2524–33. [PubMed: 16717149]

55. Takeuchi M, Nakai H, Kokumai M, Nishikage T, Otani S, Lang RM. Age-related changes in left ventricular twist assessed by two-dimensional speckle-tracking imaging. J Am Soc Echocardiogr. 2006; 19:1077–84. [PubMed: 16950461]
56. Notomi Y, Setser RM, Shiota T, Martin-Miklovic MG, Weaver JA, Popovic ZB, Yamada H, Greenberg NL, White RD, Thomas JD. Assessment of left ventricular torsional deformation by Doppler tissue imaging: validation study with tagged magnetic resonance imaging. Circulation. 2005; 111:1141–47. [PubMed: 15738351]
57. Notomi Y, Lysyansky P, Setser RM, Shiota T, Popovic ZB, Martin-Miklovic MG, Weaver JA, Oryszak SJ, Greenberg NL, White RD, Thomas JD. Measurement of ventricular torsion by two-dimensional ultrasound speckle tracking imaging. J Am Coll Cardiol. 2005; 45:2034–41. [PubMed: 15963406]
58. Takeuchi M, Borden WB, Nakai H, Nishikage T, Kokumai M, Nagakura T, Otani S, Lang RM. Reduced and delayed untwisting of the left ventricle in patients with hypertension and left ventricular hypertrophy: a study using two-dimensional speckle tracking imaging. Eur Heart J. 2007; 28:2756–62. [PubMed: 17951572]
59. Kim HK, Sohn DW, Lee SE, Choi SY, Park JS, Kim YJ, Oh BH, Park YB, Choi YS. Assessment of left ventricular rotation and torsion with two-dimensional speckle tracking echocardiography. J Am Soc Echocardiogr. 2007; 20:45–53. [PubMed: 17218201]
60. Theroux P, Franklin D, Ross J Jr, Kemper WS. Regional myocardial function during acute coronary artery occlusion and its modification by pharmacologic agents in the dog. Circ Res. 1974; 35:896–908. [PubMed: 4214626]
61. Reant P, Labrousse L, Lafitte S, Bordachar P, Pillois X, Tariosse L, Bonoron-Adele S, Padois P, Deville C, Roudaut R, Dos Santos P. Experimental validation of circumferential, longitudinal, and radial 2-dimensional strain during dobutamine stress echocardiography in ischemic conditions. J Am Coll Cardiol. 2008; 51:149–57. [PubMed: 18191740]
62. Liang HY, Cauduro S, Pellikka P, Wang J, Urheim S, Yang EH, Rihal C, Belohlavek M, Khandheria B, Miller FA, Abraham TP. Usefulness of Two-Dimensional Speckle Strain for Evaluation of Left Ventricular Diastolic Deformation in Patients With Coronary Artery Disease. Am J Cardiol. 2006; 98:1581–6. [PubMed: 17145214]
63. Geyer H, Caracciolo G, Abe H, Wilansky S, Carerj S, Gentile F, Nesser HJ, Khandheria B, Narula J, Sengupta PP. Assessment of myocardial mechanics using speckle tracking echocardiography: fundamentals and clinical applications. J Am Soc Echocardiogr. 2010; 23:351–69. [PubMed: 20362924]
64. Smalling RW, Kelley KO, Kirkeeide RL, Gould KL. Comparison of early systolic and early diastolic regional function during regional ischemia in a chronically instrumented canine model. J Am Coll Cardiol. 1983; 2:263–9. [PubMed: 6223061]
65. Yang ZR, Zhou QC, Lee L, Zou L, Zeng S, Tan Y, Cao DM. Quantitative Assessment of Left Ventricular Systolic Function in Patients with Coronary Heart Disease by Velocity Vector Imaging. Echocardiography. 2012; 29:340–5. [PubMed: 22066569]
66. Takeuchi M, Nishikage T, Nakai H, Kokumai M, Otani S, Lang RM. The assessment of left ventricular twist in anterior wall myocardial infarction using two-dimensional speckle tracking imaging. J Am Soc Echocardiogr. 2007; 20:36–44. [PubMed: 17218200]
67. Skulstad H, Edvardsen T, Urheim S, Rabben SI, Stugaard M, Lyseggen E, Ihlen H, Smiseth OA. Postsystolic shortening in ischemic myocardium: active contraction or passive recoil? Circulation. 2002; 106:718–24. [PubMed: 12163433]
68. Takayama M, Norris RM, Brown MA, Armiger LC, Rivers JT, White HD. Postsystolic shortening of acutely ischemic canine myocardium predicts early and late recovery of function after coronary artery reperfusion. Circulation. 1988; 78:994–1007. [PubMed: 3168201]
69. Holman BL, Wynne J, Idoine J, Neill J. Disruption in the temporal sequence of regional ventricular contraction. I. Characteristics and incidence in coronary artery disease. Circulation. 1980; 61:1075–83. [PubMed: 7371120]
70. Kukulski T, Jamal F, Herbots L, D'hooge J, Bijnens B, Hatle L, De Scheerder I, Sutherland GR. Identification of acutely ischemic myocardium using ultrasonic strain measurements: a clinical study in patients undergoing coronary angioplasty. J Am Coll Cardiol. 2003; 41:810–9. [PubMed: 12628727]

71. Kvitting JP, Wigström L, Strotmann JM, Sutherland GR. How accurate is visual assessment of synchronicity in myocardial motion? An in vitro study with computer-simulated regional delay in myocardial motion: clinical implications for rest and stress echocardiography studies. J Am Soc Echocardiogr. 1999; 12:698–705. [PubMed: 10477413]
72. Yu Y, Villarraga HR, Saleh HK, Cha SS, Pellikka PA. Can ischemia and dyssynchrony be detected during early stages of dobutamine stress echocardiography by 2-dimensional speckle tracking echocardiography? Int J Cardiovasc Imaging. 2013; 29:95–102. [PubMed: 22628053]
73. Mor-Avi V, Collins KA, Korcarz CE, Shah M, Spencer KT, Lang RM. Detection of regional temporal abnormalities in left ventricular function during acute myocardial ischemia. Am J Physiol Heart Circ Physiol. 2001; 280:H1770–81. [PubMed: 11247791]
74. Ishii K, Imai M, Suyama T, Maenaka M, Nagai T, Kawanami M, Seino Y. Exercise-induced post-ischemic left ventricular delayed relaxation or diastolic stunning: is it a reliable marker in detecting coronary artery disease? J Am Coll Cardiol. 2009; 53:698–705. [PubMed: 19232903]
75. Mascle S, Schnell F, Thebault C, Corbineau H, Laurent M, Hamonic S, Veillard D, Mabo P, Leguerrier A, Donal E. Predictive value of global longitudinal strain in a surgical population of organic mitral regurgitation. J Am Soc Echocardiogr. 2012; 25:766–72. [PubMed: 22609096]
76. Smedsrud MK, Pettersen E, Gjesdal O, Svennevig JL, Andersen K, Ihlen H, Edvardsen T. Detection of Left Ventricular Dysfunction by Global Longitudinal Systolic Strain in Patients with Chronic Aortic Regurgitation. J Am Soc Echocardiogr. 2011; 24:1253–9. [PubMed: 21908174]
77. Florescu M, Benea DC, Rimbas RC, Cerin G, Diena M, Lanzzillo G, Enescu OA, Cinteza M, Vinereanu D. Myocardial systolic velocities and deformation assessed by speckle tracking for early detection of left ventricular dysfunction in asymptomatic patients with severe primary mitral regurgitation. Echocardiography. 2012; 29:326–33. [PubMed: 22066959]
78. Kim MS, Kim YJ, Kim HK, Han JY, Chun HG, Kim HC, Sohn DW, Oh BH, Park YB. Evaluation of left ventricular short- and long-axis function in severe mitral regurgitation using 2-dimensional strain echocardiography. Am Heart J. 2009; 157:345–51. [PubMed: 19185644]
79. Borg AN, Harrison JL, Argyle RA, Ray SG. Left ventricular torsion in primary chronic mitral regurgitation. Heart. 2008; 94:597–603. [PubMed: 17881475]
80. Witkowski TG, Thomas JD, Delgado V, van Rijnsoever E, Ng AC, Hoke U, Ewe SH, Auger D, Yiu KH, Holman ER, Klautz RJ, Schalij MJ, Bax JJ, Marsan NA. Changes in left ventricular function after mitral valve repair for severe organic mitral regurgitation. Ann Thorac Surg. 2012; 93:754–60. [PubMed: 22296981]
81. Marciniak A, Claus P, Sutherland GR, Marciniak M, Karu T, Baltabaeva A, Merli E, Bijnens B, Jahangiri M. Changes in systolic left ventricular function in isolated mitral regurgitation. A strain rate imaging study. Eur Heart J. 2007; 28:2627–36. [PubMed: 17526904]
82. Witkowski TG, Thomas JD, Debonnaire PJ, Delgado V, Hoke U, Ewe SH, Versteegh MI, Holman ER, Schalij MJ, Bax JJ, Klautz RJ, Marsan NA. Global longitudinal strain predicts left ventricular dysfunction after mitral valve repair. Eur Heart J Cardiovasc Imaging. 2013; 14:69–76. [PubMed: 22848021]
83. Stefani L, De Luca A, Maffulli N, Mercuri R, Innocenti G, Suliman I, Toncelli L, Vono MC, Cappelli B, Pedri S, Pedrizzetti G, Galanti G. Speckle tracking for left ventricle performance in young athletes with bicuspid aortic valve and mild aortic regurgitation. Eur J Echocardiogr. 2009; 10:527–31. [PubMed: 19174444]
84. Leonardi B, Margossian R, Sanders SP, Chinali M, Colan SD. Ventricular mechanics in patients with aortic valve disease: longitudinal, radial, and circumferential components. Cardiol Young. 2013:1–8.
85. Iida N, Seo Y, Ishizu T, Nakajima H, Atsumi A, Yamamoto M, Machino-Ohtsuka T, Kawamura R, Enomoto M, Kawakami Y, Aonuma K. Transmural compensation of myocardial deformation to preserve left ventricular ejection performance in chronic aortic regurgitation. J Am Soc Echocardiogr. 2012; 25:620–8. [PubMed: 22440541]
86. Marciniak A, Sutherland GR, Marciniak M, Claus P, Bijnens B, Jahangiri M. Myocardial deformation abnormalities in patients with aortic regurgitation: a strain rate imaging study. Eur J Echocardiogr. 2009; 10:112–9. [PubMed: 18579501]

87. Olsen NT, Sogaard P, Larsson HBW, Goetze JP, Jons C, Mogelvang R, Nielsen OW, Fritz-Hansen T. Speckle-Tracking Echocardiography for Predicting Outcome in Chronic Aortic Regurgitation During Conservative Management and After Surgery. JACC: Cardiovasc Imaging. 2011; 4:223–30. [PubMed: 21414568]

88. Onishi T, Kawai H, Tatsumi K, Kataoka T, Sugiyama D, Tanaka H, Okita Y, Hirata K. Preoperative Systolic Strain Rate Predicts Postoperative Left Ventricular Dysfunction in Patients With Chronic Aortic Regurgitation. Circ Cardiovasc Imaging. 2010; 3:134–41. [PubMed: 20061517]

89. Lafitte S, Perlant M, Reant P, Serri K, Douard H, DeMaria A, Roudaut R. Impact of impaired myocardial deformations on exercise tolerance and prognosis in patients with asymptomatic aortic stenosis. Eur J Echocardiogr. 2009; 10:414–19. [PubMed: 18996958]

90. Delgado V, Tops LF, van Bommel RJ, van der Kley F, Marsan NA, Klautz RJ, Versteegh MI, Holman ER, Schalij MJ, Bax JJ. Strain analysis in patients with severe aortic stenosis and preserved left ventricular ejection fraction undergoing surgical valve replacement. Eur Heart J. 2009; 30:3037–47. [PubMed: 19726436]

91. Lindqvist P, Bajraktari G, Molle R, Palmerini E, Holmgren A, Mondillo S, Henein MY. Valve replacement for aortic stenosis normalizes subendocardial function in patients with normal ejection fraction. Eur J Echocardiogr. 2010; 11:608–13. [PubMed: 20219771]

92. Sandstede JJ, Johnson T, Harre K, Beer M, Hofmann S, Pabst T, Kenn W, Voelker W, Neubauer S, Hahn D. Cardiac systolic rotation and contraction before and after valve replacement for aortic stenosis: a myocardial tagging study using MR imaging. AJR Am J Roentgenol. 2002; 178:953–8. [PubMed: 11906882]

93. Rost C, Korder S, Wasmeier G, Wu M, Klinghammer L, Flachskampf FA, Daniel WG, Voigt JU. Sequential changes in myocardial function after valve replacement for aortic stenosis by speckle tracking echocardiography. Eur J Echocardiogr. 2010; 11:584–9. [PubMed: 20200001]

94. Takamura T, Dohi K, Onishi K, Tanabe M, Sugiura E, Nakajima H, Ichikawa K, Nakamura M, Nobori T, Ito M. Left ventricular contraction-relaxation coupling in normal, hypertrophic, and failing myocardium quantified by speckle-tracking global strain and strain rate imaging. J Am Soc Echocardiogr. 2010; 23:747–54. [PubMed: 20434880]

95. Imbalzano E, Zito C, Carerj S, Oreto G, Mandraffino G, Cusmà-Piccione M, Di Bella G, Saitta C, Saitta A. Left ventricular function in hypertension: new insight by speckle tracking echocardiography. Echocardiography. 2011; 28:649–57. [PubMed: 21676016]

96. Mizuguchi Y, Oishi Y, Miyoshi H, Iuchi A, Nagase N, Oki T. Concentric left ventricular hypertrophy brings deterioration of systolic longitudinal, circumferential, and radial myocardial deformation in hypertensive patients with preserved left ventricular pump function. J Cardiol. 2010; 55:23–33. [PubMed: 20122545]

97. Kang SJ, Lim HS, Choi BJ, Choi SY, Hwang GS, Yoon MH, Tahk SJ, Shin JH. Longitudinal strain and torsion assessed by two-dimensional speckle tracking correlate with the serum level of tissue inhibitor of matrix metalloproteinase-1, a marker of myocardial fibrosis, in patients with hypertension. J Am Soc Echocardiogr. 2008; 21:907–11. [PubMed: 18325736]

98. Goebel B, Gjesdal O, Kottke D, Otto S, Jung C, Lauten A, Figulla HR, Edvardsen T, Poerner TC. Detection of irregular patterns of myocardial contraction in patients with hypertensive heart disease: a two-dimensional ultrasound speckle tracking study. J Hypertens. 2011; 29:2255–64. [PubMed: 21946697]

99. Chen J, Cao T, Duan Y, Yuan L, Wang Z. Velocity vector imaging in assessing myocardial systolic function of hypertensive patients with left ventricular hypertrophy. Can J Cardiol. 2007; 23:957–61. [PubMed: 17932571]

100. Serri K, Reant P, Lafitte M, Berhouet M, Le Bouffos V, Roudaut R, Lafitte S. Global and regional myocardial function quantification by two-dimensional strain: application in hypertrophic cardiomyopathy. J Am Coll Cardiol. 2006; 47:1175–81. [PubMed: 16545649]

101. Popovic ZB, Kwon DH, Mishra M, Buakhamsri A, Greenberg NL, Thamilarasan M, Flamm SD, Thomas JD, Lever HM, Desai MY. Association between regional ventricular function and myocardial fibrosis in hypertrophic cardiomyopathy assessed by speckle tracking echocardiography and delayed hyperenhancement magnetic resonance imaging. J Am Soc Echocardiogr. 2008; 21:1299–305. [PubMed: 19041572]

102. Carasso S, Yang H, Woo A, Vannan MA, Jamorski M, Wigle ED, Rakowski H. Systolic myocardial mechanics in hypertrophic cardiomyopathy: novel concepts and implications for clinical status. J Am Soc Echocardiogr. 2008; 21:675–83. [PubMed: 18187306]

103. Sengupta PP, Mehta V, Arora R, Mohan JC, Khandheria BK. Quantification of regional nonuniformity and paradoxical intramural mechanics in hypertrophic cardiomyopathy by high frame rate ultrasound myocardial strain mapping. J Am Soc Echocardiogr. 2005; 18:737–42. [PubMed: 16003271]

104. Kato TS, Noda A, Izawa H, Yamada A, Obata K, Nagata K, Iwase M, Murohara T, Yokota M. Discrimination of Nonobstructive Hypertrophic Cardiomyopathy From Hypertensive Left Ventricular Hypertrophy on the Basis of Strain Rate Imaging by Tissue Doppler Ultrasonography. Circulation. 2004; 110:3808–14. [PubMed: 15583080]

105. Meluzin J, Spinarova L, Hude P, Krejci J, Poloczkova H, Podrouzkova H, Pesl M, Orban M, Dusek L, Korinek J. Left ventricular mechanics in idiopathic dilated cardiomyopathy: systolic-diastolic coupling and torsion. J Am Soc Echocardiogr. 2009; 22:486–93. [PubMed: 19345064]

106. Zeng S, Zhou QC, Peng QH, Cao DM, Tian LQ, Ao K, Liang X. Assessment of regional myocardial function in patients with dilated cardiomyopathy by velocity vector imaging. Echocardiography. 2009; 26:163–70. [PubMed: 19054025]

107. Haugaa KH, Goebel B, Dahlslett T, Meyer K, Jung C, Lauten A, Figulla HR, Poerner TC, Edvardsen T. Risk assessment of ventricular arrhythmias in patients with nonischemic dilated cardiomyopathy by strain echocardiography. J Am Soc Echocardiogr. 2012; 25:667–73. [PubMed: 22421028]

108. Tan YT, Wenzelburger F, Lee E, Heatlie G, Leyva F, Patel K, Frenneaux M, Sanderson JE. The pathophysiology of heart failure with normal ejection fraction: exercise echocardiography reveals complex abnormalities of both systolic and diastolic ventricular function involving torsion, untwist, and longitudinal motion. J Am Coll Cardiol. 2009; 54:36–46. [PubMed: 19555838]

109. Wang J, Khoury DS, Yue Y, Torre-Amione G, Nagueh SF. Preserved left ventricular twist and circumferential deformation, but depressed longitudinal and radial deformation in patients with diastolic heart failure. Eur Heart J. 2008; 29:1283–9. [PubMed: 18385117]

110. Vinereanu D, Nicolaides E, Tweddel AC, Fraser AG. “Pure” diastolic dysfunction is associated with long-axis systolic dysfunction. Implications for the diagnosis and classification of heart failure. Eur J Heart Fail. 2005; 7:820–8. [PubMed: 15921957]

111. Bertini M, Nucifora G, Marsan NA, Delgado V, van Bommel RJ, Boriani G, Biffi M, Holman ER, Van der Wall EE, Schalij MJ, Bax JJ. Left ventricular rotational mechanics in acute myocardial infarction and in chronic (ischemic and nonischemic) heart failure patients. Am J Cardiol. 2009; 103:1506–12. [PubMed: 19463507]

112. Manovel A, Dawson D, Smith B, Nihoyannopoulos P. Assessment of left ventricular function by different speckle-tracking software. Eur J Echocardiogr. 2010; 11:417–21. [PubMed: 20190272]

113. Kim DH, Kim HK, Kim MK, Chang SA, Kim YJ, Kim MA, Sohn DW, Oh BH, Park YB. Velocity vector imaging in the measurement of left ventricular twist mechanics: head-to-head one way comparison between speckle tracking echocardiography and velocity vector imaging. J Am Soc Echocardiogr. 2009; 22:1344–52. [PubMed: 19828287]

114. Biaggi P, Carasso S, Garceau P, Greutmann M, Gruner C, Tsang W, Rakowski H, Agmon Y, Woo A. Comparison of two different speckle tracking software systems: does the method matter? Echocardiography. 2011; 28:539–47. [PubMed: 21517954]

115. Seo Y, Ishizu T, Enomoto Y, Sugimori H, Yamamoto M, Machino T, Kawamura R, Aonuma K. Validation of 3-dimensional speckle tracking imaging to quantify regional myocardial deformation. Circ Cardiovasc Imaging. 2009; 2:451–9. [PubMed: 19920043]

116. Yodwut C, Weinert L, Klas B, Lang RM, Mor-Avi V. Effects of Frame Rate on Three-Dimensional Speckle-Tracking-based Measurements of Myocardial Deformation. J Am Soc Echocardiogr. 2012; 25:978–85. [PubMed: 22766029]

117. Saito K, Okura H, Watanabe N, Hayashida A, Obase K, Imai K, Maehama T, Kawamoto T, Neishi Y, Yoshida K. Comprehensive evaluation of left ventricular strain using speckle tracking echocardiography in normal adults: comparison of three-dimensional and two-dimensional approaches. J Am Soc Echocardiogr. 2009; 22:1025–30. [PubMed: 19556106]

118. Bansal M, Cho GY, Chan J, Leano R, Haluska BA, Marwick TH. Feasibility and Accuracy of Different Techniques of Two-Dimensional Speckle Based Strain and Validation With Harmonic Phase Magnetic Resonance Imaging. J Am Soc Echocardiogr. 2008; 21:1318–25. [PubMed: 19041575]
119. Pirat B, Khoury DS, Hartley CJ, Tiller L, Rao L, Schulz DG, Nagueh SF, Zoghbi WA. A novel feature-tracking echocardiographic method for the quantitation of regional myocardial function: validation in an animal model of ischemia-reperfusion. J Am Coll Cardiol. 2008; 51:651–9. [PubMed: 18261685]
120. Sun JP, Lee AP, Wu C, Lam YY, Hung MJ, Chen L, Hu Z, Fang F, Yang XS, Merlino JD, Yu CM. Quantification of left ventricular regional myocardial function using two-dimensional speckle tracking echocardiography in healthy volunteers - A multi-center study. Int J Cardiol. 2013; 167:495–501. [PubMed: 22365315]
121. Kuznetsova T, Herbots L, Richart T, D'hooge J, Thijs L, Fagard RH, Herregods MC, Staessen JA. Left ventricular strain and strain rate in a general population. Eur Heart J. 2008; 29:2014–23. [PubMed: 18583396]
122. Risum N, Ali S, Olsen NT, Jons C, Khouri MG, Lauridsen TK, Samad Z, Velazquez EJ, Sogaard P, Kisslo J. Variability of global left ventricular deformation analysis using vendor dependent and independent two-dimensional speckle-tracking software in adults. J Am Soc Echocardiogr. 2012; 25:1195–203. [PubMed: 22981228]
123. Nelson MR, Hurst RT, Raslan SF, Cha S, Wilansky S, Lester SJ. Echocardiographic measures of myocardial deformation by speckle-tracking technologies: the need for standardization? J Am Soc Echocardiogr. 2012; 25:1189–94. [PubMed: 22981227]
124. Koopman LP, Slorach C, Manlhiot C, McCrindle BW, Jaeggi ET, Mertens L, Friedberg MK. Assessment of myocardial deformation in children using Digital Imaging and Communications in Medicine (DICOM) data and vendor independent speckle tracking software. J Am Soc Echocardiogr. 2011; 24:37–44. [PubMed: 21095099]
125. Patrianakos A, Kalogerakis A, Zacharaki A, Nyktari EA, Psathakis E, Parthenakis FI, Vardas PE. Comparison of peak longitudinal systolic strain normal values, using 2D-strain echocardiography with 2 different high-end ultrasound systems. Eur J Echocardiography Abstracts Supplement. 2012; 13(S1):il21.

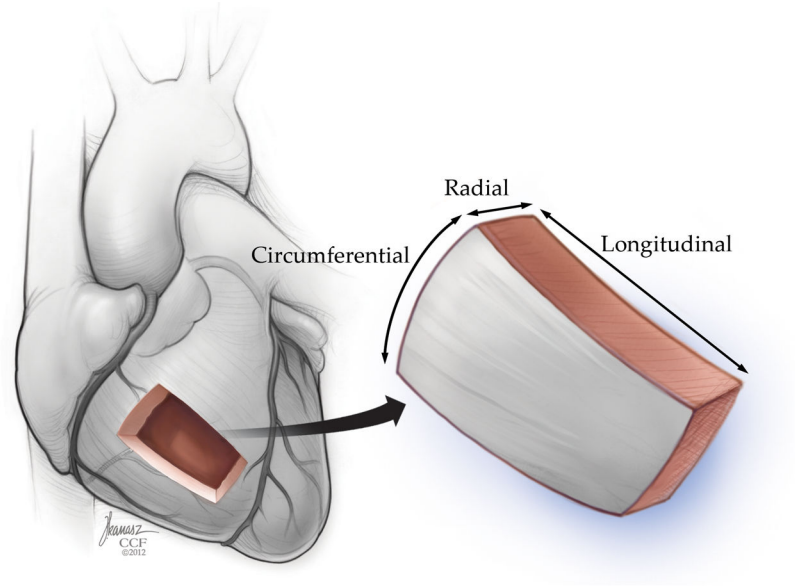


**Figure 1.**

Myocardial deformation occurs in the longitudinal (base to apex), radial (or “transverse”), and circumferential dimension (encircling the short-axis of the ventricle). “Reprinted with permission, Cleveland Clinic Center for Medical Art & Photography © 2013. All Rights Reserved.”

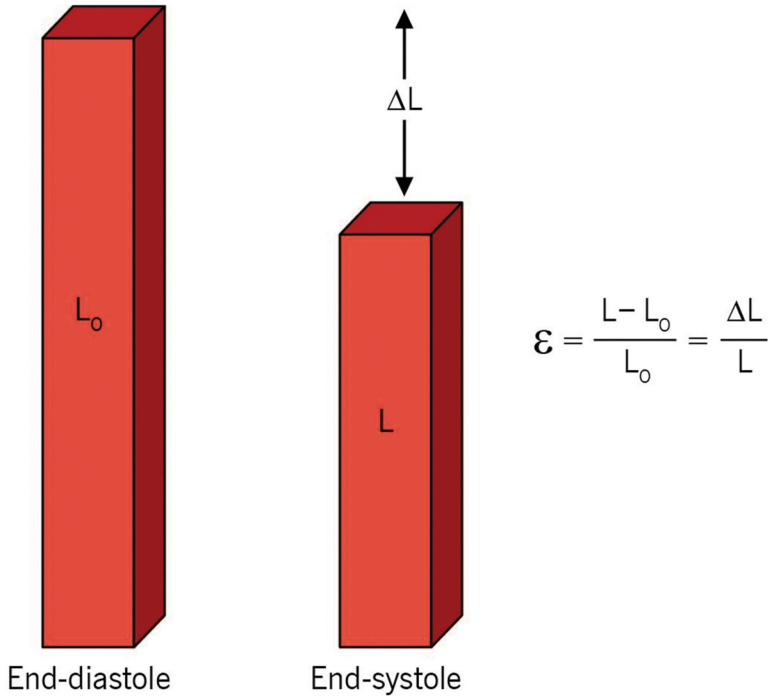


**Figure 2.**

Strain describes fractional change of a myocardial segment length compared to its initial length (at end-diastole). ε =myocardial strain, L =length at end-systole, $L_0$ =initial length. "Reprinted with permission, Cleveland Clinic Center for Medical Art & Photography © 2013. All Rights Reserved."

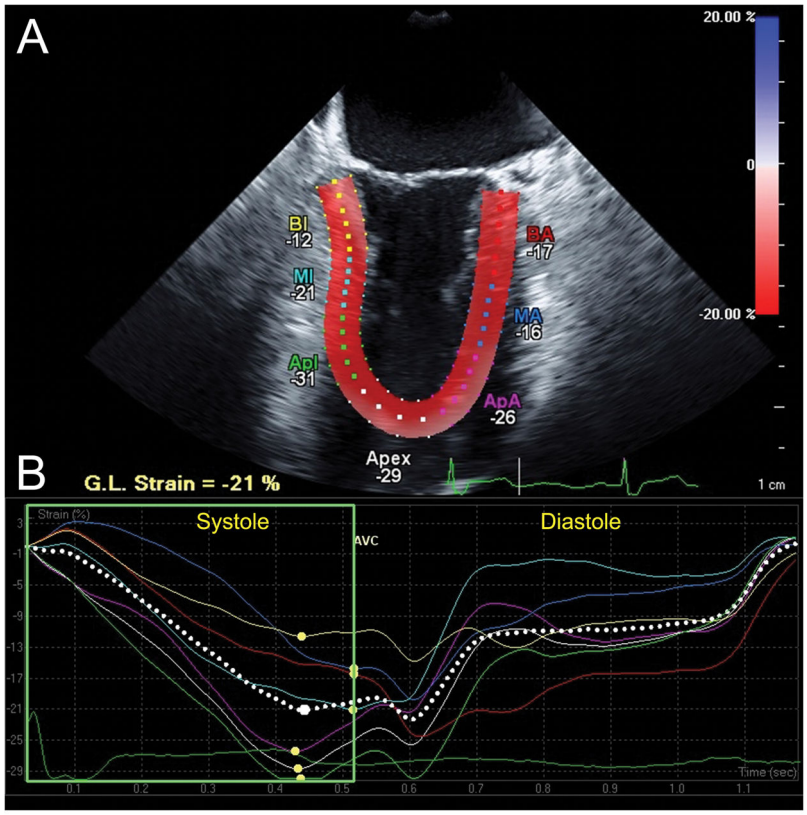


**Figure 3.**

Longitudinal strain analysis assessed with Cardiac Motion Quantification (CMQ) (Philips Medical Systems, Andover, MA). (A) Mid-esophageal two-chamber echocardiographic view depicting the left ventricle (LV), where the myocardial walls are divided into six segments distinguished by color-coded labels and dots. Segmental strain measurements are shown adjacent to each segment. The myocardium is colored in shades of red corresponding to percent longitudinal shortening (strain) measured by the red-to-blue scale on the upper right-hand side. (B) Longitudinal strain curves, which are color-coded to correspond to myocardial segments in panel A, with time on the X-axis relative to the cardiac cycle and percent shortening (strain) on the Y-axis, demonstrate shortening during systole and returning to baseline at end-diastole. The pink curve, for example, represents the apical anterior wall which experiences peak shortening of −26% during systole (yellow dot identifies *peak systolic strain*). In contrast, *end-systolic strain*, measured at time of aortic valve closure (AVC), measures −23%, demonstrating that peak strain may differ from end-systolic strain. The dotted white curve represents global longitudinal strain. BA =Basal anterior; MA =Mid anterior; ApA =Apical anterior, BI =Basal inferior; MI = Mid inferior; Apl =Apical Inferior myocardial walls. G.L. Strain =Global longitudinal strain. AVC =aortic valve closure. “Reprinted with permission, Cleveland Clinic Center for Medical Art & Photography © 2013. All Rights Reserved.”

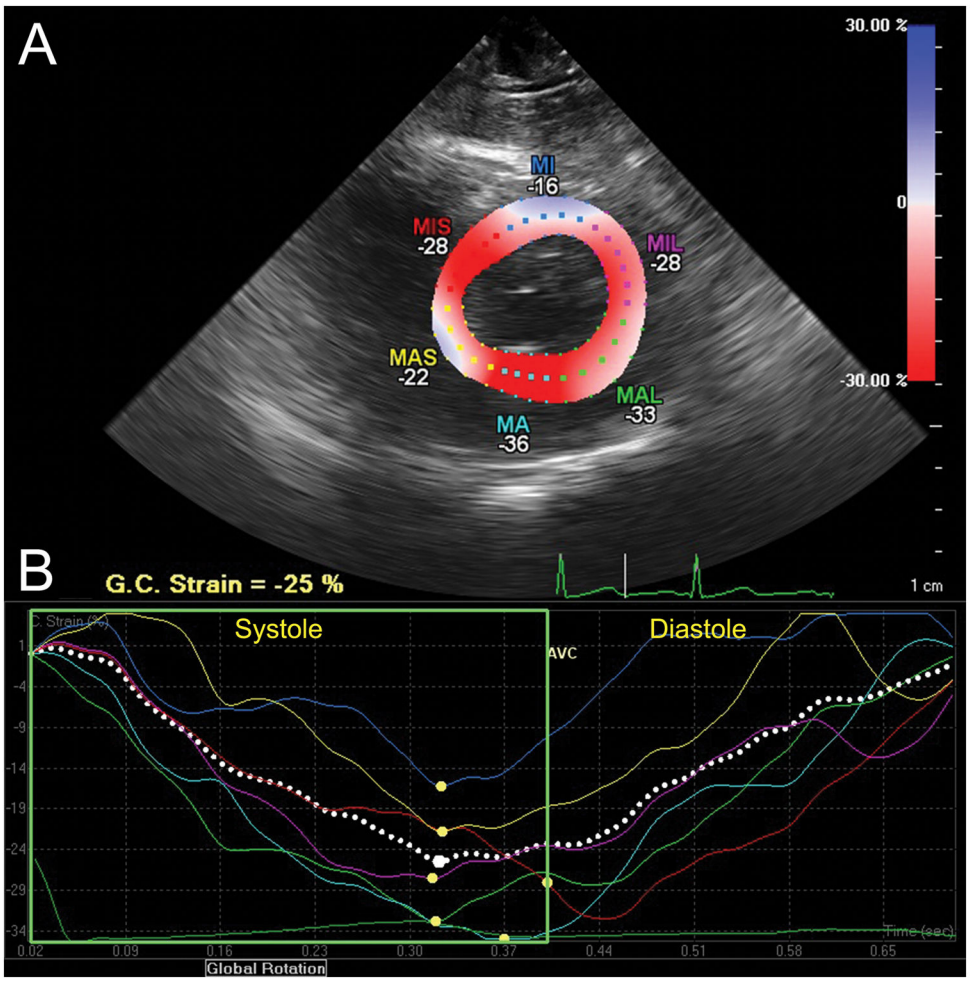


**Figure 4.**

Circumferential strain analysis assessed with CMQ. (A) This transgastric midpapillary short-axis view of the LV is divided into six segments distinguished by color-coded labels and dots. Segmental strain measurements are shown adjacent to each segment. The myocardium is colored in shades of red-to-blue according to the scale on the right-hand side demonstrating the percent circumferential shortening (strain). (B) Circumferential strain curves, with time on the X-axis and percent shortening (strain) on the Y-axis corresponding to similarly color-coded myocardial segments in panel A, demonstrate shortening during systole and return to baseline at end-diastole. Peak systolic circumferential strain is marked by a yellow dot.

G.C. Strain = Global circumferential strain; MIS =Mid-inferoseptal; MI =mid-inferior; MIL =Mid-inferolateral; MAL =Mid-anterolateral; MA =Mid-anterior; MAS =Mid-anteroseptal wall. “Reprinted with permission, Cleveland Clinic Center for Medical Art & Photography © 2013. All Rights Reserved.”

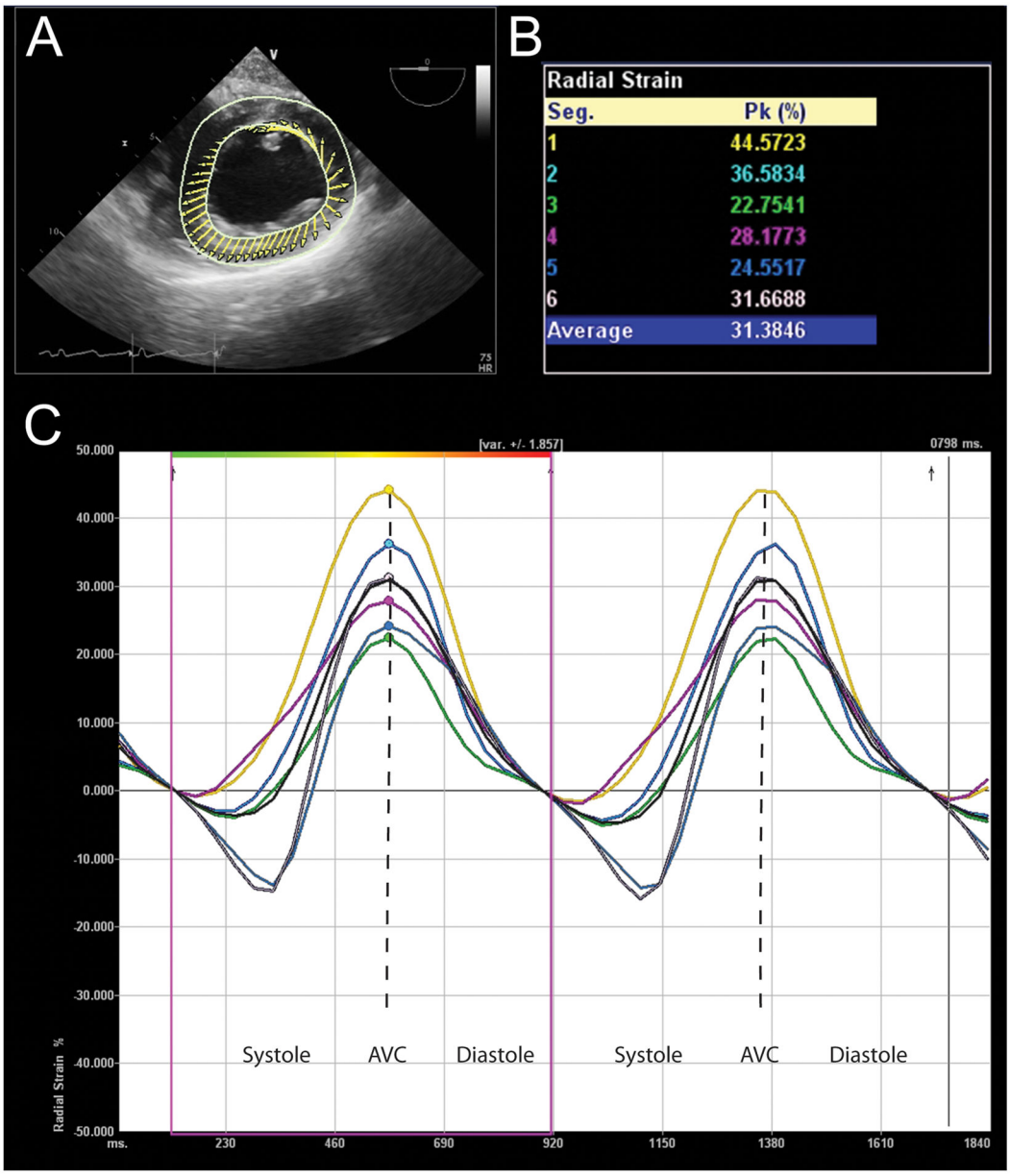


**Figure 5.**

Radial strain analysis assessed with Velocity Vector Imaging (VVI) (Siemens Medical Solutions, Malvern, PA). (A) This transgastric midpapillary short-axis echocardiographic view depicts the LV, where the direction and relative length of arrows demonstrate direction and amplitude of myocardial velocities. (B) Peak radial strain for six myocardial segments is displayed in this table. (C) Strain curves of two cardiac cycles with time on the X-axis and percent radial strain on the Y-axis. These curves are color-coded to correspond to the myocardial segment described in similarly colored text in Panel B. Peak radial strain is identified with a similarly colored dots. Please note that radial strain is positive since the ventricle thickens in the radial direction.

AVC = aortic valve closure. “Reprinted with permission, Cleveland Clinic Center for Medical Art & Photography © 2013. All Rights Reserved.”

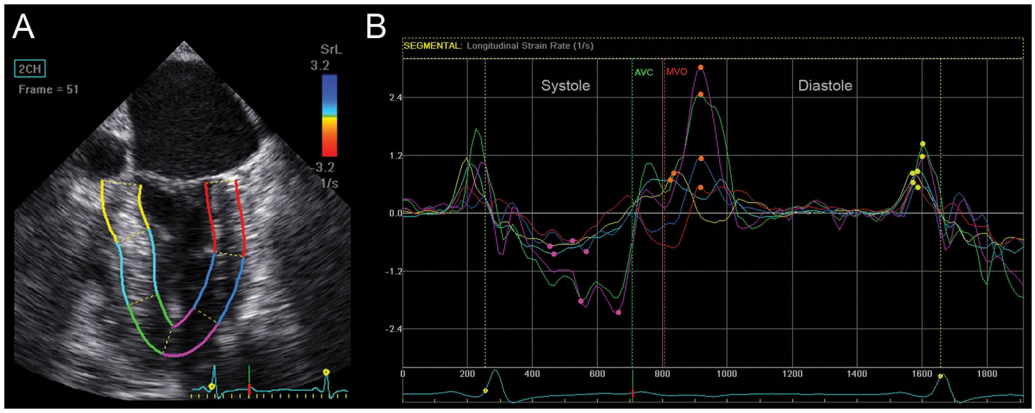


**Figure 6.**

Strain rate (SR) analyses assessed with EchoPAC (GE Healthcare, Horten, Norway). (A) LV in this mid-esophageal commissural view is divided into six color-coded myocardial segments. (B) Longitudinal SR curves corresponding to similarly colored myocardial segments in panel A are shown. The rate of longitudinal systolic shortening is demonstrated by a negative SR curve. Peak systolic SR is labeled with a pink dot. Following peak systolic SR, the SR curve returns toward zero at time of aortic valve closure (AVC) followed by a biphasic curve during isovolumetric relaxation (between AVC and mitral valve opening (MVO)). Phases of diastole are demonstrated as peak early diastolic SR ($SR_E$), labeled with an orange dot, and late diastolic SR ($SR_A$), corresponding to atrial contraction and marked with a yellow dot. Diastasis, a relatively flat portion of the curve between early and late diastole, has a SR near zero. 

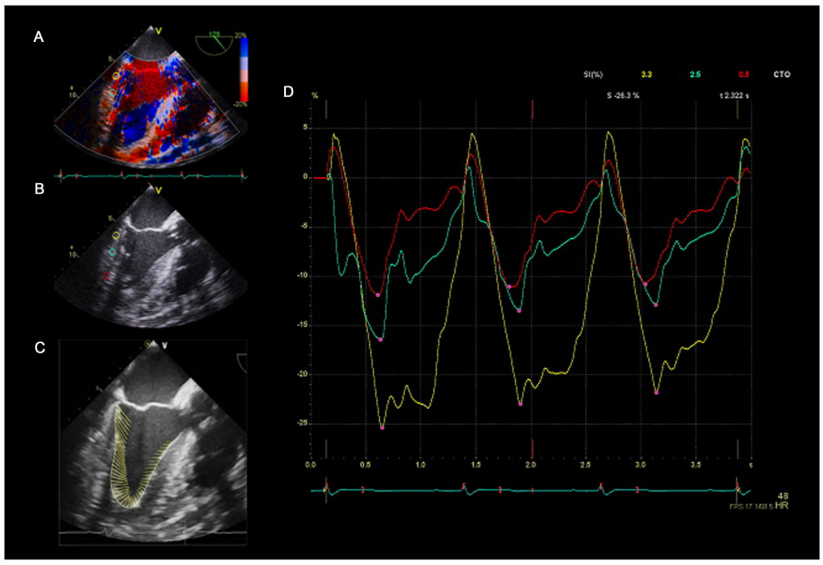


**Figure 7.**

Tissue Doppler imaging (TDI) strain. (A) A mid-esophageal long-axis view with color tissue Doppler. (B) The operator positions three sample volumes (yellow, aqua, and red circles) within the inferolateral wall to measure TDI strain at each point. (C) Demonstration of the myocardial vector of motion using VVI strain analysis software documents suboptimal alignment with the ultrasound beam. D) Strain curves from the “encircled” region in panel B are shown in the corresponding color. Three cardiac cycles are shown, and peak systolic strain for each region is identified by a pink dot. The “red” sample volume positioned nearest to the apex demonstrates the lowest strain because of poor alignment of the region of interest and vector of motion with the ultrasound beam. “Reprinted with permission, Cleveland Clinic Center for Medical Art & Photography © 2013. All Rights Reserved.”

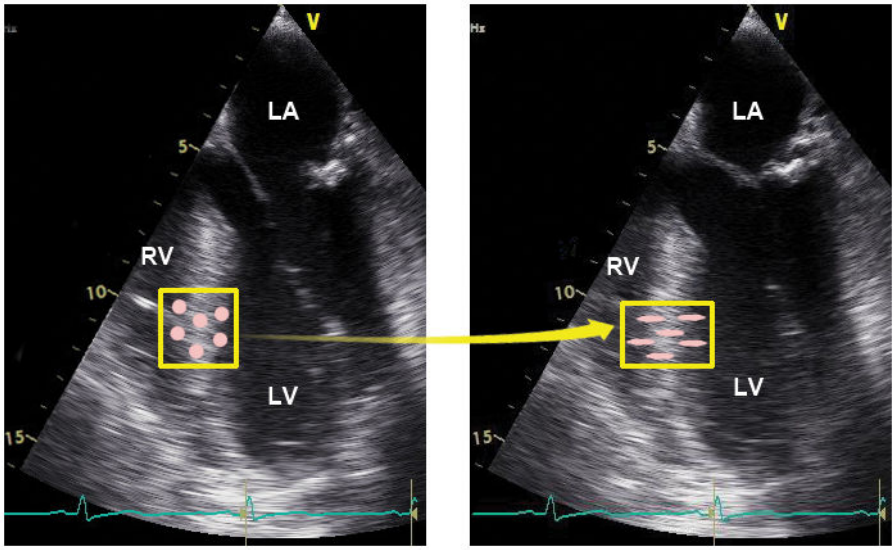


**Figure 8.**

Myocardial deformation measured by speckle-tracking echocardiography tracks myocardial movement and deformation using the speckles in echocardiographic images. These sequential echocardiographic frames provide an example of the tracking of a unique pattern or “fingerprint” in the myocardial region of interest (yellow box) from frame-to-frame to measure myocardial deformation. The pink circles within the box represent myocardial speckles, which experience shortening in the longitudinal direction and thickening in the transverse direction. RV =right ventricle, LV =left ventricle, LA =left atrium. “Reprinted with permission, Cleveland Clinic Center for Medical Art & Photography © 2013. All Rights Reserved.”

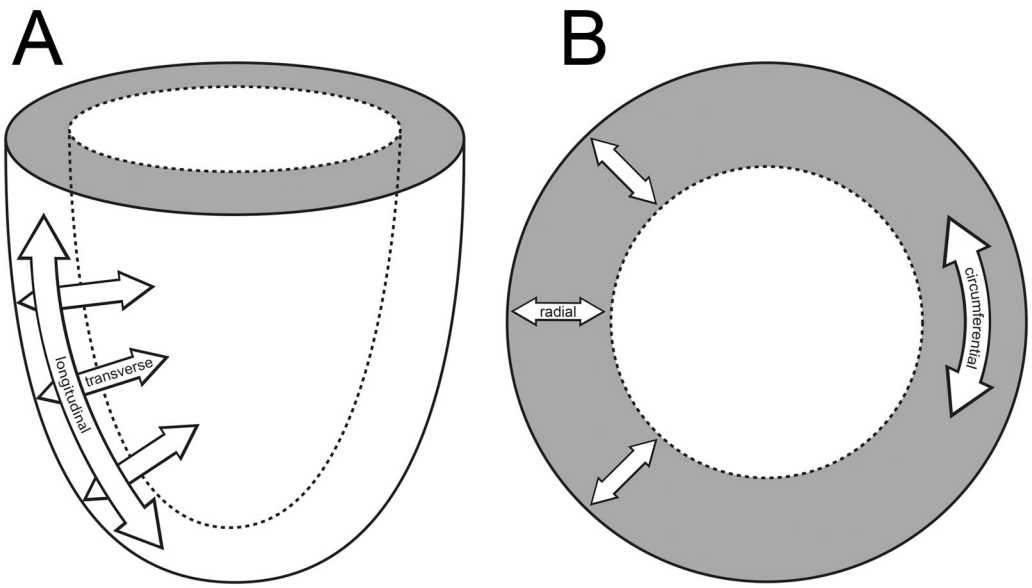


**Figure 9.**

A. Long-axis views of the left ventricle measure longitudinal (shortening) and transverse (thickening) strain. B. Short-axis views of the left ventricle measure circumferential (shortening around the circular LV) and radial (thickening) strain. “Reprinted with permission, Cleveland Clinic Center for Medical Art & Photography © 2013. All Rights Reserved.”

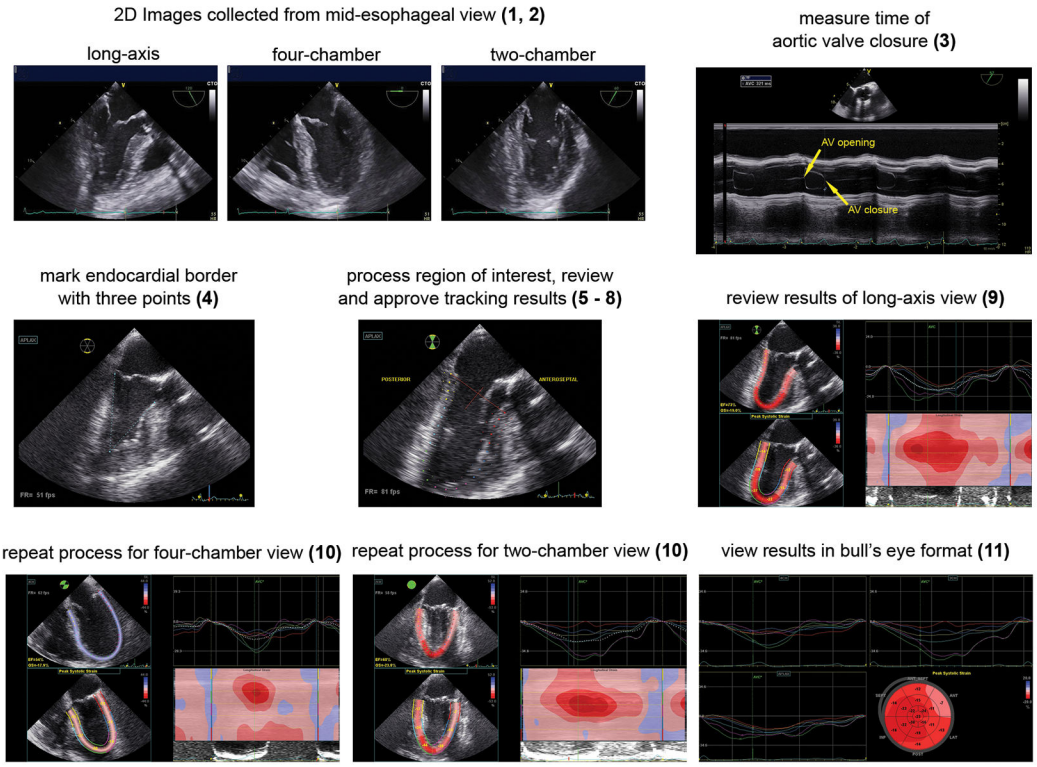


**Figure 10.**

Acquisition of longitudinal strain using speckle-tracking echocardiography. Optimal 2D mid-esophageal long-axis, four-chamber, and two-chamber images are collected (1, 2). M-mode of the aortic valve determines time of aortic valve closure (3). In the long-axis view, the endocardial border is marked (4). The region of interest is processed, reviewed, and approved by the operator (5–8). Results of strain analysis are reviewed. The strain analysis includes strain curves, peak segmental strain values superimposed on the LV, and a color M-mode display, which demonstrates myocardial deformation over time according to the red-to-blue scale (9). The process is repeated for the four- and two-chamber views (10). LV longitudinal strain values from the three mid-esophageal views are shown in a bull's eye view (11). The numbers in parenthesis correspond to steps listed in Table 2. "Reprinted with permission, Cleveland Clinic Center for Medical Art & Photography © 2013. All Rights Reserved."

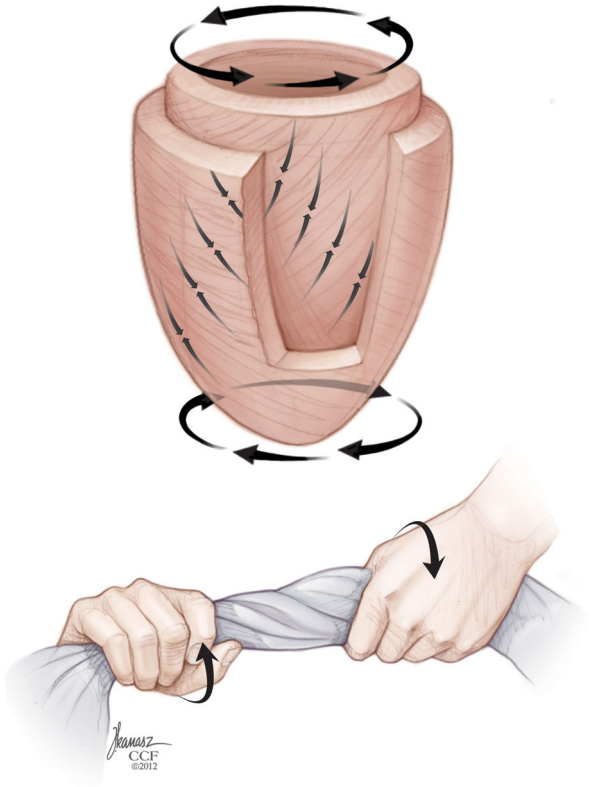


**Figure 11.**

Model of LV myofiber structure and twist mechanics. The contractile motion of the LV is dictated by the spiral structure of the myocardial fibers. Subendocardial myofibers are wrapped in a right-handed helix, sub-epicardial fibers are wrapped in a left-handed helix, and mid-myocardial fibers are oriented parallel to the circumferential direction. Following a brief clockwise rotation of the apex and opposite (counterclockwise) rotation of the base during isovolumic contraction, the subendocardial and subepicardial fibers shorten concurrently during ejection, causing a “wringing” motion of the apex and base in counterclockwise and clockwise directions, respectively, when viewed from the apex. “Reprinted with permission, Cleveland Clinic Center for Medical Art & Photography © 2013. All Rights Reserved.”

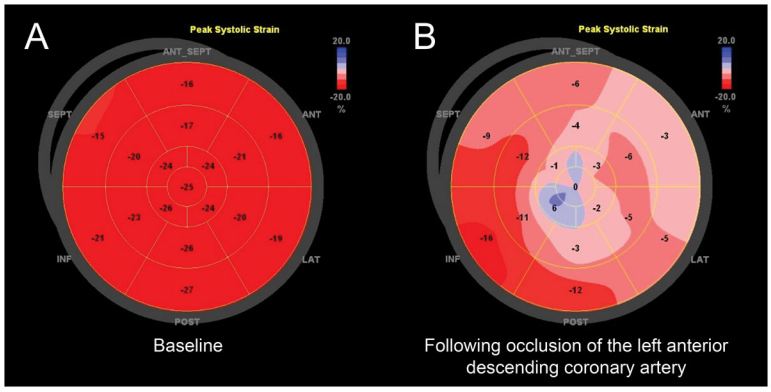


**Figure 12.**

Bull's eye views depicting longitudinal strain measurements from the animal laboratory measured with transthoracic echocardiography. A red-to-blue scale in the upper right hand corner of each panel represents percent strain, where greater percent shortening is shown as a darker shade of red. Lengthening (dyskinesis) is displayed in shades of blue. (A) Normal LV function in a dog at baseline. (B) Severe anterior, anteroseptal, anterolateral, and apical wall motion abnormalities in a dog following acute occlusion of the left anterior descending coronary artery. "Reprinted with permission, Cleveland Clinic Center for Medical Art & Photography © 2013. All Rights Reserved."

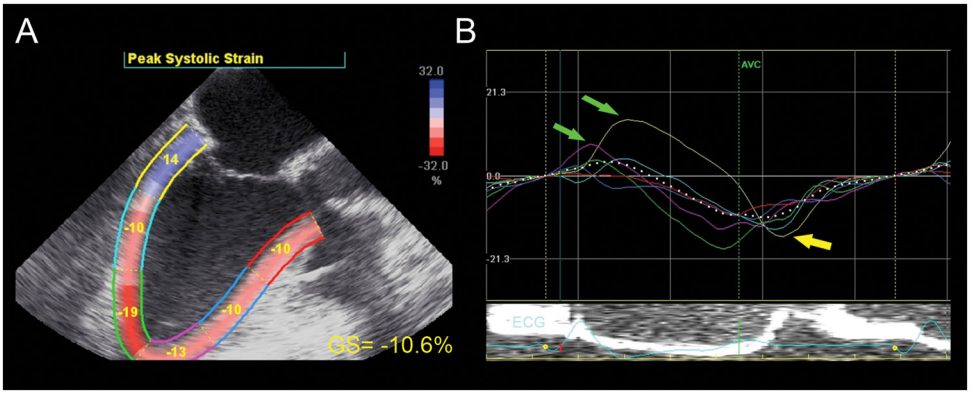


**Figure 13.**

Strain analysis. (A) This mid-esophageal long-axis view depicts the left ventricle divided into six color-coded myocardial segments. Each segment is labeled with its peak strain measurement. Global longitudinal strain (GS) is abnormal (−10.6%). (B) Post-systolic strain, or “postsystolic shortening” can be seen in the basal (yellow curve) and mid-inferolateral (light blue curve) myocardial wall (yellow arrow). Pre-stretch in the basal inferolateral (yellow) and apical anteroseptal (pink) myocardial region is also seen (green arrows). AVC =aortic valve closure; GS =global strain. “Reprinted with permission, Cleveland Clinic Center for Medical Art & Photography © 2013. All Rights Reserved.”

## Table 1

Definitions

| | |
|---|---|
| Strain (ε; %) | The proportional change in myocardial length between end-diastole and end-systole $\varepsilon = (L - L_0)/L_0 = \Delta L/L_0$ |
| End-systolic strain (%) | Strain measured at end-systole (defined as the time of aortic valve closure) |
| Peak systolic strain (%) | Strain measured at time of greatest systolic deformation |
| Global strain (%) | Average strain for all myocardial segments |
| Pre-stretch | Brief lengthening of myocardial segment in early systole prior to systolic shortening |
| Post-systolic shortening (or post-systolic strain) | Peak strain occurring in early diastole |
| Strain Rate (SR; $sec^{-1}$) | Change in strain per unit time $SR = \Delta\varepsilon/\Delta t,$ |
| Rotation (degrees) | Degrees of LV rotation viewed from the apex |
| LV twist (degrees) | Rotation of the apex relative to the base, or, the absolute apex-to-base difference in rotation |
| Torsion (degrees per centimeter) | Apex-to-base gradient in the rotation angle of the LV long axis where the twist angle is divided by the distance between base and apex |

LV = Left ventricle; ε = strain; L= length at end-systole; $L_0$ = initial length measured at end-diastole; t = time (seconds); SR = strain rate

## Table 2

Image acquisition for strain analysis with speckle-tracking echocardiography

| Strain measurement | Step | Action | Comment |
|---|---|---|---|
| Longitudinal strain | 1 | Optimize echocardiographic image and adjust settings | Narrow image sector, adjust frame rate between 40 and 90 fps, adjust settings to record three heart beats. |
| | 2 | Collect a mid-esophageal 4-chamber, 2-chamber, and long-axis view | Ensure the ventricle is seen in entirety throughout the cardiac cycle. Optimize visualization of the endocardium. Heart rate needs to be similar (within10 beats/min) in all views |
| | 3 | Record time of aortic valve closure | Use 2D long axis view, CW Doppler or M-mode through aortic valve |
| | 4 | In midesophageal long-axis view, tracking of the endocardial border is performed by placement of markers by the operator to identify the region of interest | EchoPak, CMQ require only three points (endocardial borders of mitral and aortic annulus and apex). Exclude ventricular trabeculae from the region of interest. |
| | 5 | Process image | The software will “track” the ventricle |
| | 6 | Review tracking results | Critically review the tracking of the region of interest to ensure that the region of interest follows true ventricular deformation. Adjust width of the region of interest to the thickness of the myocardium. |
| | 7 | Readjust tracking of the myocardial segments if necessary | Most software programs allow adjustment of the endocardial border/myocardium by a click and “pull” process. |
| | 8 | “Accept” tracking when the overlay tracing appears true to ventricular deformation | |
| | 9 | Review strain analysis results | Strain curves, peak strain values, and a color M-mode display, which demonstrate ventricular deformation over time according to the red-to-blue scale, are shown |
| | 10 | Repeat process for the 4-chamber and 2-chamber views | |
| | 11 | If available, select bull’s eye view | Software programs, including EchoPAC, CMQ, will combine peak strain results from all three views into a “bull’s eye” plot |
| Radial and Circumferential strain | 12 | Collect transgastric mid-papillary LV short-axis view | Optimize visualization of the endocardium. Confirm the short-axis image is circular and not an oblique cut |
| | 13 | Determine aortic valve closure time | May already be entered from above analysis |
| | 14 | Trace endocardial border | |
| | 15 | Process image | The software will “track” the ventricle |
| | 16 | Review tracking results | Critically review the tracking of the ventricle by ensuring that the overlay tracing follows true ventricular deformation |
| | 17 | Readjust tracking of myocardial segments if necessary | Most software programs allow you to adjust the endocardial border/myocardium by a click and “pull” process. |
| | 18 | “Accept” tracking when the overlaid tracing appears true to ventricular deformation | Strain results will be shown |

LV = Left ventricle

**Table 3**

Software options for strain analysis.

| Vendor | Software | Vendor-specific | Ultrasound machine | Comment |
|---|---|---|---|---|
| GE Healthcare Vingmed Ultrasound AS, Horten, Norway | Automated Function imaging (AFI), EchoPAC | Yes | Vivid 7 and Vivid E9 | Speckle-tracking; validated with HARP-MRI[118] |
| Philips Healthcare, Andover, MA | Cardiac Motion Quantification (CMQ), QLab | Yes | Philips iE33 | Speckle-tracking |
| Siemens Medical Solutions, Mountain View, CA | Velocity Vector Imaging | No | Standard 2D B-mode clips | Feature-tracking (speckle-tracking with incorporation of endocardial border); validated with sonomicrometry.[119] |
| Toshiba Medical Systems, Tokyo, Japan | 2D Wall Motion Tracking | Yes | Artida and Aplio | Speckle-tracking |
| TomTec Imaging Systems, Munich, Germany | 2D Cardiac Performance Analysis | No | Standard 2D B-mode clips | Speckle-tracking |
| Epsilon Imaging, Ann Arbor, MI | EchoInsight | No | Any ultrasound system. | Proprietary tissue-tracking technology applied to radio-frequency and speckle data; uses raw data rather than B-mode images; allows adjustment of the components of measurement |

**Table 4**

"Normal values" for longitudinal, circumferential, and radial strain measured by transthoracic echocardiography with various ultrasound systems and software analysis packages. Data is presented as mean ± SD.

| Author | Approach | Subjects | Longitudinal Strain | Circumferential Strain | Radial strain |
|---|---|---|---|---|---|
| Yingchoncharoen et al.[39] | Meta-analysis of 24 studies using various ultrasound systems and speckle-tracking software | 2597 subjects from 24 studies | −19.7 ± 0.4% | −23.3 ± 0.7% | 47.3 ± 1.9% |
| Manovel et al.[112] | Vivid 7 with EchoPAC (GE Healthcare, Horten, Norway), speckle-tracking | 28 healthy subjects (age 38 ± 12) | −21.95 ± 1.8% | −23.18 ± 3.3% | 46.97 ± 5.5% |
| Manovel et al.[112] | Artida 4D and 2D Wall Motion tracking (Toshiba Medical Systems), speckle tracking | 28 healthy subjects (age 38 ± 12) | −22.28 ± 2.1% | −27.17 ± 4.7% | 40.74 ± 4.3% |
| Marwick et al.[18] | Vivid 7 with EchoPAC (GE Healthcare, Horten, Norway), speckle-tracking | 242 healthy subjects | −18.6 ±1.6% | | |
| Dalen et al.[31] | Vivid 7 (GE Healthcare), combination of TDI and speckle tracking | 1266 free from DM or CV disease | −17.4 ± 2.3% (females)<br>−15.9% ± 2.3% (males) | | |
| Dalen et al. [31] | Vivid 7 with Automated Function Imaging (GE Healthcare), combination of TDI and speckle tracking | 57 subjects free from cardiovascular disease | −17.4 ± 3.4% | | |
| Dalen et al. [31] | Vivid 7 (GE Healthcare), TDI with fixed Region of Interest | 57 subjects free from cardiovascular disease | −17.7 ± 8.5% | | |
| Dalen et al. [31] | Vivid 7 and Automated Function Imaging (GE Healthcare), speckle-tracking | 57 subjects free from cardiovascular disease | −18.4 ± 5.9% | | |
| Sun et al.[120] | Vivid 7 (GE Healthcare), Speckle-tracking | 228 healthy subjects | −20.4 ± 3.4% | −22.9 ± 3.1% | 42.6±12.9% |
| Kuznetsova et al.[121] | Vivid 7 and EchoPAC (GE Healthcare), TDI strain | 480 subjects from a general population | −22.9 ± 1.9% | | 59.2 ± 2.5% |

## Table 5

Investigations comparing various strain analysis software programs.

| Study | Subjects | Ultrasound system | Strain analysis software package | Results |
|---|---|---|---|---|
| Risum et al.[122] | 15 healthy and 15 subjects with cardiac disease | GE Vivid E9 or Philips iE33 | EchoPAC (GE Vingmed Ultrasound AS) and 2D Cardiac Performance Analysis (TomTec Imaging Systems, Numich, Germany) | Longitudinal strain had highest reproducibility; Circumferential and radial strain had lower reproducibility; EchoPAC had lower variability compared with 2D Cardiac Performance Analysis |
| Nelson et al.[123] | 100 patients without atrial arrhythmias | Vivid 7 (GE Vingmed Ultrasound AS, Horten, Norway) | EchoInsight (Epsilon, Ann Arbor, MI) vs. Image-Arena (TomTec Imaging Systems, Unterschleissheim, Germany) | Strain with Image-Arena was more negative; adjustment of components of measurement with EchoInsight resulted in more similar strain measurements |
| Manovel et al[112] | 28 healthy subjects | Vivid 7 (GE) and Artida 4D (Toshiba Medical Systems) | EchoPAC vs. 2D Wall Motion Tracking (Toshiba) | Global longitudinal strain was similar between EchoPAC and 2D Wall Motion Tracking; limits of agreement were larger for radial and circumferential strain |
| Sun et al.[120] | 52 healthy subjects | Vivid 7 (GE) and iE33 (Philips) | EchoPAC vs. QLab (Philips) | Strain measured with QLab were 10% higher than measures from GE system |
| Bansal et al.[118] | 30 patients with ischemic heart disease | Vivid 7 (GE) | AFI/EchoPAC vs. VVI; Tagged harmonic phase (HARP) magnetic resonance imaging (MRI) as reference standard | VVI and AFI underestimated longitudinal strain compared with HARP-MRI; AFI strain measurements were more strongly correlated with HARP MRI compared with VVI |
| Koopman et al.[124] | 34 children with or without heart disease | Vivid 7 (GE) and iE33 (Philips) | Vendor-specific software (EchoPAC, QLAB) and vendor-independent software (Cardiac Performance Analysis, Tomtec Imaging Systems) | Longitudinal strain values were comparable between vendor-independent and vendor-specific software.<br>Circumferential strain was higher with vendor-independent software.<br>radial strain measured by vendor independent software was lower than measured by EchoPAC and higher than values measured with QLAB |
| Biaggi et al.[114] | 47 healthy subjects | Vivid 7 (GE) | EchoPAC vs. VVI | Longitudinal strain gradients were similar between software packages, however, peak segmental strain in longitudinal, circumferential, and radial directions differed significantly between software |
| Patrianakos et al.[125] | 37 volunteers | Vivid 7 (GE) and iE33 (Philips) | EchoPAC vs. QLab | GE and Philips echo stations provided similar cut-off values for longitudinal systolic strain associated with LVEF > 50% |

**Table 6**

Changes in strain, strain rate, and twist in cardiovascular disease. "↓" denotes a decrease, "↑" denotes an increase (usually a compensatory response), and "↔" denotes no change. Because the literature has contradictory findings, "any" denotes the fact that strain is reported to be increased, decreased, or maintained.

| Disease | Strain | | | Strain rate | Twist or Untwist |
|---|---|---|---|---|---|
| | Longitudinal | Radial | Circumferential | | |
| Coronary Artery Disease | ↓ (early) | ↓ | ↓ or normal | ↓ (all directions) | normal or ↓ |
| Valve disease | | | | | |
| Aortic regurgitation | ↓ (early) | any (early)<br>↓ (late) | any (early)<br>↓ (late) | ↓ (all directions) | |
| Mitral regurgitation | ↓ | ↓ | | ↓ (all directions) | normal or ↓ untwisting |
| Aortic stenosis | ↓ | ↓ or normal (early)<br>↓ (late) | ↓ (late) | ↓ (longitudinal) | normal or ↑ twist |
| Hypertension | ↓ (early) | ↓ | normal or ↑<br>↓ (late) | ↓ all directions (late) | any |
| Cardiomyopathy | | | | | |
| Hypertrophic cardiomyopathy | ↓ | ↓ | ↓ | ↓(longitudinal) | ↔ twist, ↓ untwist |
| Nonischemic dilated cardiomyopathy | ↓ | ↓ | ↓ | ↓(all directions) | abnormal |
| Diastolic and systolic heart failure | ↓ (early) | ↑ (early)<br>↓ (late) | ↑ (early)<br>↓ (late) | | normal or ↑ (early)<br>↓ (late) |